Multi-fold increase in rainforests tipping risk beyond 1.5-2°C warming

Chandrakant Singh[1,2,3,*], Ruud van der Ent[4], Ingo Fetzer[1,2,5], Lan Wang-Erlandsson[1,2,5]

[1]Stockholm Resilience Centre, Stockholm University, Stockholm, Sweden
[2]Bolin Centre for Climate Research, Stockholm University, Stockholm, Sweden
[3]Department of Space, Earth and Environment, Chalmers University of Technology, Gothenburg, Sweden
[4]Department of Water Management, Faculty of Civil Engineering and Geosciences, Delft University of Technology, Delft, The Netherlands
[5]Potsdam Institute for Climate Impact Research, Potsdam, Germany

*Corresponding author; E-mail: chandrakant.singh@su.se, chandrakant.singh@chalmers.se

ORCID
Chandrakant Singh: http://orcid.org/0000-0001-9092-1855
Ruud van der Ent: https://orcid.org/0000-0001-5450-4333
Ingo Fetzer: http://orcid.org/0000-0001-7335-5679
Lan Wang-Erlandsson: http://orcid.org/0000-0002-7739-5069

Abstract. Tropical rainforests ~~invest~~ rely ~~in~~ on their root systems to access ~~store~~ moisture stored in soil ~~in their root zone from~~ during ~~water-rich~~ wet periods for use ~~in~~ during ~~water-scarce~~ dry periods. When this root-zone soil moisture is ~~An~~ inadequate to sustain a ~~root zone soil moisture storage predisposes or forces these~~ forest ecosystem~~s~~, they ~~to~~ transition to a savanna-like state, losing ~~devoid of~~ their native structure and functions. Yet the influence of climate change on ecosystem's root-zone soil moisture storage and their impact on rainforest ecosystems ~~changes in soil moisture storage and its influence on the rainforest ecosystems under future climate change~~ remain uncertain. This study assesses the future state of rainforests and the risk of forest-to-savanna transitions in South America and Africa under four shared socioeconomic pathways (SSP1-2.6, SSP2-4.5, SSP3-7.0, and SSP5-8.5). Using ~~the~~ a (mass-balance-based~~)~~ empirical understanding of root zone storage capacity (S_r), defined as the maximum volume of root zone soil moisture per unit area accessible to vegetation's roots for transpiration, we project how rainforest ecosystems will respond to future climate changes. ~~, we assess the future state of the rainforests and the forest-to-savanna transition risk in South America and Africa under four different shared socioeconomic pathway scenarios.~~ We find that under the end-of-the-21st-century climate, nearly one-third of the total forest area will be influenced by climate change.~~.~~ ~~Furthermore~~As the climate warms~~, beyond 1.5-2°C warming~~, forests will require a larger S_r than they do under the current climate to sustain their ecosystem structure and functions, making them more water-limited~~ecosystem~~. Meanwhile, recover~~ing to a less water-limited state~~y gradually ~~reduces~~diminishes~~-~~. Furthermore, warming beyond 1.5-2°C will significantly elevate the ~~whereas the~~ risk of a forest-savanna transition~~ risk increases several folds~~. In the

Formatted

37 Amazon, the forest area at risk of such a transition grows by about 1.7-5.8 times in size compared to their
38 immediate lower warming scenario (e.g., SSP2-4.5 compared to SSP1-2.6). In contrast, the risk growth in the
39 Congo is less substantial, ranging from 0.7-1.7 times. For Amazon, this risk can grow by about 1.5-6 times
40 compared to its immediate lower warming scenario, whereas for Congo, this risk growth is not substantial (0.7-
41 1.65 times). These insights from this study underscores the urgent need to limit global surface temperature rise
42 below the Paris Agreement to conserve rainforest ecosystems and associated ecosystem services.

1 Introduction

Tropical rainforests in the Amazon and Congo basins are critical to the Earth system since they store and sequester a large amount of carbon, host vast biodiversity, and regulate the global water cycle (Malhi et al., 2014). However, these forests are under severe pressure from climate change and land-use change (Davidson et al., 2012; Lewis et al., 2015; Malhi et al., 2008), which risk amplifying further warming and forest degradation (Lawrence et al., 2022). Climate change and land-use change lead to a decrease in precipitation, an increase in seasonality and atmospheric water demand (Malhi et al., 2014). This causes a deficit in soil moisture availability that inhibits plant growth (Singh et al., 2020; Wang-Erlandsson et al., 2022). Furthermore, climate-induced hydroclimatic changes, including the projected increases in drought frequency, severity, and duration (Dai, 2011; Liu et al., 2018), present imminent threats to the capacity of rainforests to maintain their native ecological structure and functions (i.e., forest resilience) (Bauman et al., 2022; Grimm et al., 2013; Jones et al., 2009).

Under water-deficit conditions, rainforests adapt by investing in their root systems to ~~increase~~ gain better ~~their capacity to~~ access ~~to~~ soil moisture necessary to maintain their structure and functions (Singh et al., 2020, 2022). At the same time, the availability of surplus moisture at shallow depths minimises the need for ecosystems to invest in extensive (deeper and lateral) root systems (Bruno et al., 2006). Furthermore, forest ecosystems adapt to climate change by optimising water distribution through mechanisms such as hydraulic redistribution (Liu et al., 2020; Oliveira et al., 2005), enhancing water-use efficiency by regulating stomatal conductance, and even shredding leaves (Wolfe et al., 2016) to minimise moisture loss (Barros et al., 2019; Brum et al., 2019; Lammertsma et al., 2011). Despite their critical role, the dynamic influence of climate change on vegetation's rooting structure and subsoil moisture is challenging to measure at the ecosystem scale (Fan et al., 2017). Thus, understanding how moisture from wet periods is stored, transmitted, and lost from soil, and how it is accessed by vegetation during dry periods, is critical to the ecohydrology and resilience of terrestrial ecosystems under climate change~~Since the rooting structure is challenging to measure at the ecosystem scale (Fan et al., 2017),~~. ~~previous studies have found that empirical mass balance-derived root zone storage capacity (S$_r$) correlates well with ecosystems' capacity to store water in its roots and their above ground transition dynamics (de Boer-Euser et al., 2016; Singh et al., 2020; Stocker et al., 2023; Wang-Erlandsson et al., 2016) – thus serves as a proxy for ecosystems ability to store, utilize and adapt based on available subsoil moisture. Here, S$_r$ constitutes a hydrological buffer required by the ecosystem for the collection of surplus precipitation from wet periods to be stored and used for evaporation throughout the dry periods (when total evaporation is greater than precipitation) (Grossiord et al., 2020; Singh et al., 2020; Wang-Erlandsson et al., 2016). Therefore, a lowly water-stressed (defined based on the magnitude of deficit in soil moisture availability inhibiting plant growth) ecosystem will need the least investment to access stored moisture.~~

~~In contrast, a highly water-stressed ecosystem will require extensive subsoil investment (Singh et al., 2020). However, S$_r$ investment is costly, and there exists a ceiling up to where ecosystems cannot maximise~~

Field Code Changed

3

77 ~~their *S* any further (Singh et al., 2020, 2022a). Approaching this ceiling also implies that forest ecosystems are~~
78 ~~depleting their adaptive capacity towards further future hydroclimatic changes (Fan et al., 2017; Guswa, 2008;~~
79 ~~Kleidon and Heimann, 1998; Singh et al., 2020), with forests that have extended their *S* close to their maximum~~
80 ~~storage limit being most vulnerable to increases in water-stress (Singh et al., 2022a). Excessive short-term water~~
81 ~~deficits in these forests lead to tree mortality, loss of carbon sink strength, and an increase in the risk of fire~~
82 ~~(Aleixo et al., 2019; Bauman et al., 2022; van Nes et al., 2018; Singh et al., 2022b), whereas long-term water~~
83 ~~deficits can lead to large-scale tipping to a savanna-like state (Hirota et al., 2011; Staal et al., 2020; Staver et al.,~~
84 ~~2011; Zemp et al., 2017).~~

85

86 However, such ecohydrological dynamics remain challenging to incorporate in ~~the~~ Earth System Models
87 (ESMs) (Lenton, 2011; Maslin and Austin, 2012; Valdes, 2011) – complex mathematical representations of Earth
88 system processes and interactions across different biospheres. This limits ESM's capacity to simulate tipping
89 points as an emergent property of the system (i.e., properties that emerge due to multiple interactions between
90 several system components, and ~~is~~ are not the property of an individual component) (Hirota et al., 2021; Reyer
91 et al., 2015). This constraint is mainly due to our poor understanding of complex mechanisms governing the
92 ecosystem, which are not well represented in ESMs. This includes a limited understanding of vegetation-climate
93 feedbacks (Boulton et al., 2013, 2017; Chai et al., 2021), subsoil moisture availability (Cheng et al., 2017),
94 adaptation dynamics (Yuan et al., 2022), the response time of forest ecosystems to climate change
95 perturbations, and assumptions about future (i.e., prescribed) land-use change (Hurtt et al., 2020) in the ESMs.
96 Furthermore, in the Earth system, some interactions still remain largely unknown, thereby making the
97 prediction of (abrupt) forest-to-savanna transition (referring to changes in the dense-canopy structure of
98 forests to one that mimics an open-canopy structure similar to savanna; hereafter referred to as forest-savanna
99 transition) challenging (Drijfhout et al., 2015; Hall et al., 2019; Koch et al., 2021).

100 To understand the extent of rainforest tipping risks, there is a need to assess and contrast the forest
101 resilience consequences of low-emission and current commitment trajectories with the more commonly used
102 high-emission scenario (Jehn et al., 2022). ~~In addition~~However, the risk of forest-savanna transitions under
103 various possible climate future scenarios is relatively under-investigated. As a result of the conflicting findings
104 and scenario-dependent uncertainties, the Intergovernmental Panel on Climate Change (IPCC) has only low
105 confidence about the possible tipping of the Amazon forest by the end of the 21st century (Canadell et al., 2021).
106 However, with mounting empirical evidence on how climate change influences rainforest ecosystems (Boulton
107 et al., 2022; Küçük et al., 2022; Singh et al., 2020, 2022), the research on rainforest resilience loss has
108 accelerated considerably in the recent decade (Ahlström et al., 2017; Huntingford et al., 2013). Yet, forest
109 resilience is often assessed based on changes in forest carbon stocks (Huntingford et al., 2013; Parry et al.,
110 2022) or precipitation (Hirota et al., 2011; Staal et al., 2020; Zemp et al., 2017); and rarely on the subsoil ~~actual~~

4

111 moisture ~~storage capacity in the root zone~~availability of the ecosystem (Singh et al., 2022). ~~Further, there is a~~
112 ~~need to assess and contrast the forest resilience consequences of low-emission and current commitment~~
113 ~~trajectories with the more commonly used high-emission scenario (Jehn et al., 2022).~~
114 This study aims to assess the state of rainforests ~~resilience~~ and the risk of a forest-savanna transition ~~by~~
115 under the end of the ~~21st~~ 21st-century climate based on an empirical understanding of ecosystems' root zone
116 storage dynamics. For this, we use ~~hydroclimate~~mass-balance- derived root zone storage capacity (S_r) –
117 representing the maximum amount of soil moisture vegetation can access for transpiration (Gao et al., 2014;
118 Singh et al., 2020; Wang-Erlandsson et al., 2016)~~– to classify the ecosystems under current and future climates,~~
119 ~~and assess potential forest transitions~~. Our use of S_r is grounded in its effectiveness in representing ecosystems'
120 access to soil moisture and their ability to modify above-ground structures accordingly (de Boer-Euser et al.,
121 2016; Singh et al., 2020; Stocker et al., 2023; Wang-Erlandsson et al., 2016). It should be noted that we refer to
122 rainforest tipping as a forest-savanna transition 'risk' since the timing of such transitions depends on the
123 stochastic fluctuations of other environmental factors, beyond just hydroclimate (e.g., fire, human influence,
124 species composition) (Cole et al., 2014; Cooper et al., 2020; Higgins and Scheiter, 2012; Poorter et al., 2016).
125 Therefore, to project if an ecosystem is a forest or has tipped to savanna in the future, we assume the
126 hydroclimate projected by the end of the 21st century (i.e., 2086-2100) and ecosystem are in equilibrium.
127 However, we do not account for the time required for ecosystems to reach their (long-term) equilibrium state,
128 which previous studies suggest can take between 50-200 years after crossing the tipping point (Armstrong
129 McKay et al., 2022).
130
131

132 ## 2 Methodology

133 ### 2.1 Study Area

134 This study focuses on forest ecosystems (i.e., excluding savanna/grassland and vegetation in human-influenced
135 ecosystems) extending between 15°N–35°S for South America and Africa.
136

137 ### 2.2 Data

138 This analysis uses both empirical and ESM-simulated datasets of precipitation and evaporation. Empirical
139 datasets include remotely sensed and observation-corrected precipitation and evaporation time-series.
140 Empirical precipitation estimates at daily timestep are obtained from the Climate Hazards Group InfraRed
141 Precipitation with Station data (CHIRPS; 0.25° resolution) (Funk et al., 2015). Furthermore, empirical
142 evaporation is derived using an equally-weighted ensemble of three different datasets – (i) Breathing Earth
143 System Simulator (BESS; 0.5° resolution) (Jiang and Ryu, 2016) (ii) Penman-Monteith-Leuning (PML; 0.5°
144 resolution) (Zhang et al., 2016) and (iii) FLUXCOM-RS (0.083° resolution) (Jung et al., 2019) – at monthly

145 timestep. Here, evaporation represents the sum of all evaporated moisture from the soil, open water and
146 vegetation, including interception and transpiration. We only selected evaporation datasets free from biome-
147 dependent parameterisation (such as plant function types, stomatal conductance, and maximum root
148 allocation depth) and soil layer depth (represents maximum depth of moisture uptake). Ultimately, all
149 evaporation datasets are bilinearly interpolated to 0.25^o resolution and downscaled to daily timestep using
150 ERA5 evaporation (0.25^o resolution) estimates (Hersbach et al., 2020). All empirical datasets are obtained for
151 2001-2012.

152 We also obtained precipitation and evaporation estimates from 33 ESMs (from 22 different institutes),
153 which includes CMIP6-historical and four SSP scenario simulations (SSP1-2.6 leads to approx. 1.3-2.4^{o}C
154 warming; SSP2-4.5 corresponds to 2.1-3.5^{o}C warming and is closest to the current trajectory according to the
155 nationally determined contributions (Anon, 2015); SSP3-7.0 around 2.8-4.6^{o}C warming; and SSP5-8.5
156 represents 3.3-5.7^{o}C warming; ^{o}C warming represents an increase in mean global surface temperature change
157 by the end of 21st century relative to 1850-1900 (IPCC, 2021) (Fig. 1; ~~Supplementary~~ Table S1 and S2). The
158 historical estimates are obtained at a monthly timestep for 2000-2014, and the estimates under different SSPs
159 are obtained for 2086-2100. Though obtained estimates from different ESMs are at different spatial resolutions,
160 we bilinearly interpolated them to 0.25^o for this analysis.

161 Finally, to minimise the influence of human activity and non-forest land cover on the natural water cycle,
162 we utilised land-cover data to remove pixels with such features from our analysis. We began by removing
163 human-influenced and non-forest land cover, such as savanna, grasslands, and water bodies, from Globcover,
164 a global land-cover classification dataset by the European Space Agency (ESA) at 300m resolution (GlobCover
165 land-use map, 2022). We then performed majority interpolation to convert the dataset to a 0.25^o resolution
166 and to mask grid cells with less than 50% forest cover. This step ensured that only grid cells with over 50% forest
167 cover were classified as forests for further analysis.

168
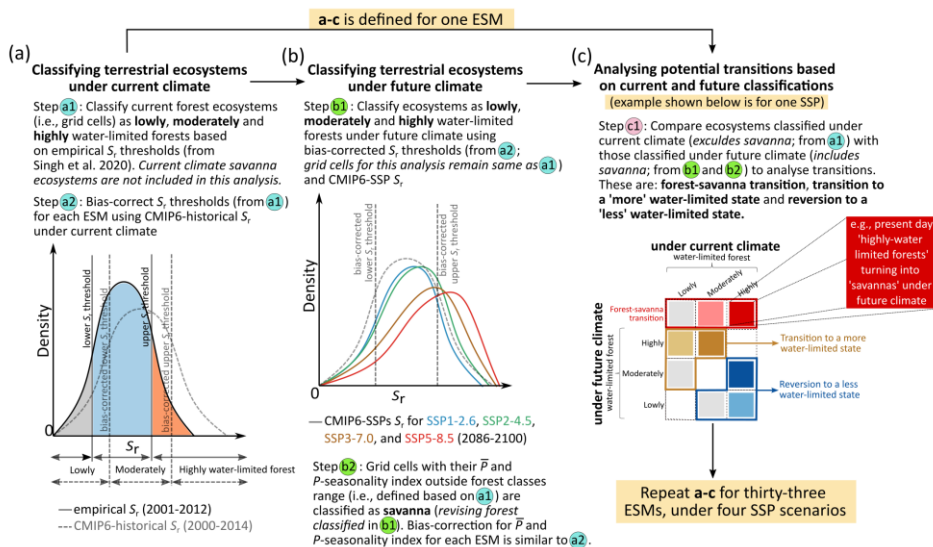
Figure 1: Methodological framework for analysing the potential transitions in tropical terrestrial ecosystems using empirical and CMIP6-Earth System Models (ESMs) hydroclimate estimates. (a) We use root zone storage capacity (S_r)-based classification thresholds (obtained from Singh et al., 2020) − calculated using empirical precipitation (P) and evaporation (E) estimates (~~Supplementary~~ Fig. S1; see ~~Methods~~ Methodology section and Appendix A1) − to classify terrestrial ecosystems under the current climate. Savanna ecosystems under the current climate are excluded from this analysis. We bias-correct these S_r thresholds for all ESMs using the histogram equivalence method (Piani et al., 2010) (~~Supplementary~~ Table S1). (b) We then use these bias-corrected S_r thresholds to classify ecosystems under future climate conditions (~~Supplementary~~ Figs. S2− and S3). Furthermore, we use mean annual precipitation ($\bar{P}$) and P-seasonality index range (S_r-based forest classes from a) − as a proxy for ecosystem state − to revise our classification under future climate (Appendix A3 and ~~Supplementary~~ Fig. S4). (c) We then analyse the potential transitions by comparing ecosystems classified under the current climate (analysed in a) with those classified under future climate (analysed in b) individually for all ESMs (~~Supplementary~~ Figs. S5− and S6 ~~and Supplementary Data~~). The transition analysis assumes that the vegetation and hydroclimate are in equilibrium, and does not account for the time required for transitions to occur. A detailed description is provided in the Methodology ~~Methods~~ section ~~section~~. An exemplification of this methodological framework is shown in ~~Supplementary~~ Fig. S7.

2.3   Root zone storage capacity-based framework for projecting forest transitions

~~Previous studies have shown that forest ecosystems adapt to water deficit by investing in roots to store and access subsoil water (Brum et al., 2019; Fan et al., 2017; Nepstad et al., 1994), efficiently distribute water through their roots for transpiration during dry periods (e.g., hydraulic redistribution) (Liu et al., 2020; Oliveira et al., 2005), maximise water use efficiency (by regulating stomatal conductance) or minimise moisture loss (by shredding leaves (Wolfe et al., 2016)) to reduce root zone moisture storage (Barros et al., 2019; Brum et al., 2019; Lammertsma et al., 2011). Since v~~Vegetation uptakes soil moisture from its roots; thus, the availability of root zone ~~available~~ moisture is a key element that mediates the interaction between vegetation and climate

(Brooks et al., 2015; Küçük et al., 2022; Rosas et al., 2019; Wang-Erlandsson et al., 2022). However, measuring soil- (such as texture and porosity) and root-characteristics (such as vertical and lateral extent and soil moisture uptake profiles) that influence access to subsoil moisture are challenging to measure at ecosystem scales (Bruno et al., 2006). Furthermore, land-system models tend to oversimplify the transfer and storage of water in ~~roots~~ root-zone due to insufficient knowledge about soil-vegetation-climate interactions (Albasha et al., 2015; Hildebrandt et al., 2016; Wang et al., 2004). In such cases, the mass-balance approach-based S_r provides a tangible and comprehensive understanding of ecosystem access to ~~subsoil dynamics~~ moisture stored in the soil (de Boer-Euser et al., 2016; Gao et al., 2014; McCormick et al., 2021; Stocker et al., 2023).

2.3.1 Estimating mass-balance derived ~~Root~~ root zone storage capacity (S$_r$)

Derived using the mass-balance approach, S_r represents the maximum amount of soil moisture accessed by vegetation for transpiration (Singh et al., 2020; Wang-Erlandsson et al., 2016). This methodology calculates the maximum ~~This~~ extent of soil moisture ~~is stored~~ within the reach of plant roots, ~~eyond This methodology~~ assum~~inges~~ that ecosystems do not invest in expanding their root-zone storage beyond what is ~~more than~~ necessary to bridge the maximum (accumulated) water-deficit experienced by the vegetation ~~in~~ during dry periods (i.e., periods in which evaporation is greater than rainfall, irrespective of the seasons). This ~~the~~ maximum annual accumulated water deficit ($D_{a,y}$) experienced by the ecosystem is calculated using daily precipitation and evaporation estimates (Appendix A1 and Fig. A1). Subsoil moisture beyond the reach of plant roots is primarily controlled by gravity-induced gradients (de Boer-Euser et al., 2016) and is not available for transpiration. ~~It is, thus, independent of any prior vegetation, soil, or land cover based, ithydroclimatic estimates (and Fig. A1)~~ information (Wang-Erlandsson et al., 2016). The rationale is that ~~Since investment requires carbon allocation,~~ any extensive investment (i.e., more than necessary) in root expansion ~~will~~ would require carbon allocation and, thus, is inefficient from the perspective of the plants (Gao et al., 2014; Schenk, 2008). Since, this approach does not rely on prior information about vegetation, soil, or land cover-based, by ~~This mass-balance approach only requires precipitation and evaporation estimates to determine S_r. It is, thus, independent of any prior vegetation, soil or land cover based information (Wang-Erlandsson et al., 2016). Furthermoreerefore,~~ using empirical (observation-based) datasets (Appendix A1 and Fig. A1), we capture the dynamics of ~~actual state of the ecosystems — reflecting the~~ actual soil moisture ~~availabil~~availableity for the ecosystems (Wang-Erlandsson et al., 2016)~~(Singh et al., 2020)~~. The detailed methodology for calculating S_r using precipitation and evaporation estimates is outlined in Appendix A1.

In this mass-balance approach, S_r only represents a hydrological buffer essential for maintaining the ecosystem's structure and functions (Gao et al., 2014; Wang-Erlandsson et al., 2016). However, other biotic and abiotic factors, such as root morphology, soil depth, and geological formations, can physically restrict S_r by limiting rooting depth, rooting structure, and the soil's water-holding capacity (Canadell et al., 1996; Jackson et

8

229 al., 1996; Schenk and Jackson, 2002) (Appendix A2). Additionally, soil properties like porosity or field capacity

230 could necessitate a deeper rooting strategy in different soil types (e.g., between sandy and clayey soil) to

231 achieve a comparable level of S_r to sustain the ecosystem under future climate (Kukal and Irmak, 2023).

232 However, this study assesses the impact of future climate change on the ecosystem's hydrological regime,

233 focusing on the changes to the ecosystem's equilibrium state. Therefore, the direct influence of soil and root

234 characteristics under future climate change on S_r (Appendix A2) and forest transitions falls outside our current

235 scope.

236

2.3.2   Determining root zone storage capacity thresholds for forest transitions

238 Previous empirical studies on mass-balance derived S_r have provided a comprehensive understanding of

239 catchment characteristics and the ecosystem's subsoil dynamics (de Boer-Euser et al., 2016; Gao et al., 2014).

240 However, aA recent study by Singh et al. (2020) demonstrated that found them S_r effectively represents an

241 ecosystem's above-ground state (i.e., whether it is a forest or savanna) and its level of water-stress, based on

242 root-zone moisture availabilityto dynamically represent the ecosystem's above-ground structure and below-

243 ground root zone adaptation dynamics. In this study, we refine their terminology from 'water-stressed state' to

244 'water-limited state' to more precisely describe the effects of hydroclimatic conditions on forest ecosystems,

245 specifically in terms of inhibiting plant growth based on subsoil moisture availability and the potential of them

246 approaching the threshold of forest-savanna transition. According to Singh et al. (2020), in response to water-

247 limited conditions, forests adapt their rooting strategies and modify their above-ground forest cover. These

248 adaptations aim to allocate carbon in the most efficient way possible to maximise the hydrological benefits

249 available to the ecosystem. They classified terrestrial ecosystems into four distinct categories based on the

250 relationship between tree cover density and root zone storage capacity (S_r), illustrating the various drought

251 coping strategies of ecosystems (detailed description provided in (Singh et al., 2020):

i. **Lowly water-limited forest:** Dense forests (>70% tree cover) that receive ample rainfall (with daily

253   precipitation exceeding evaporation year-round) results in a very low $D_{p,y}$. In such an environment, the

254   top layer of the soil remains consistently damp, allowing for efficient soil moisture uptake through

255   shallow roots (<1m; S_r and maximum rooting depth comparison in Singh et al., 2020), as vegetation

256   typically utilises the shortest available pathway for moisture uptake (Bruno et al., 2006). Consequently,

257   these forest ecosystems can sustain themselves with a low S_r (<100 mm).e

ii. **Moderately water-limited forest:** Although these forests retain a dense structure (>65% tree cover),

259   the increased precipitation seasonality (evaporation rates remain same as before) leads to a relatively

260   higher $D_{o,y}$. This necessitates a greater investment in their rooting systems to access subsoil moisture

261   for dry periods, with S_r for these ecosystems ranging between 100-400 mm in South America and 100-

9

262 350 mm in Africa. Notably, this enhanced below-ground investment does not compromise the above-

263 ground ecosystem structure. ~~sit can withing~~

264 iii. **Highly water-limited forest:** With further increase in precipitation seasonality (even negligible

265 precipitation during dry seasons) and duration of dry period, forests need to maximize their S_r

266 (maximum rooting depths typically between 15-20m). Maintaining ecosystems under these conditions

267 is costly from a subsoil investment perspective (Schenk, 2008), with regions in South America and Africa

268 showing S_r values as high as 750 mm and 450 mm, respectively. Consequently, these values represent

269 the upper limits beyond which forest ecosystems cannot further enhance their S_r.

270 Possible mechanisms suggest that these trees adapt by shedding leaves to minimise

271 moisture loss (Wolfe et al., 2016). However, this adaptation can reduce photosynthetic activity, leading

272 to declines in root growth ~~(Guswa, 2008)~~, and heightening the risk of mortality from hydraulic failures

273 due to the unavailability of soil moisture at accessible depths (Guswa, 2008). Furthermore,

274 accumulation of dry leaves also perpetuates forest fires, thinning the ecosystem even further (tree

275 cover can drop as low as 30%) (Nepstad et al., 1999). Although increased tree mortality reduces

276 competition for water, enabling some trees to survive, the heightened risk of hydraulic failures and

277 forest fires makes these ecosystems highly susceptible to transitioning to savanna.

278 iv. **Savanna-grassland regime** (hereafter referred to as **savanna**): These ecosystems, typically

279 characterised by an open, grass-dominated structure (tree cover <40%), have both a lower water

280 availability and demand (both precipitation and evaporation are lower than in forest ecosystems). Thus,

281 requiring a lower hydrological buffer to sustain their structure and functions. For these ecosystems, S_r

282 values can be as low as 100 mm. Although tree species in this ecosystem can develop deep roots

283 (extending up to 20m) ~~(Nippert and Holdo, 2015; Schenk, 2008)~~, the majority of the root biomass is

284 concentrated in the shallow soil layers (top 30–50 cm; shallow water uptake profile) (Nippert and

285 Holdo, 2015; Schenk, 2008). This strategy allows for completive moisture uptake between trees and

286 grass species. This also suggests that, for savanna, deeper roots don't always necessitate a high S_r.

287

288 The difference in S_r thresholds between both continents is due to the presence of water-use-efficient

289 C4 grasses in Africa (Still et al., 2003), which reduces the competitiveness for moisture uptake between tree

290 species and grasses – leading to a lesser need for extensive S_r in the African forest ecosystem (Singh et al., 2020),

291 ==and validated against empirical rooting depth (Fan et al., 2017) and ecoregion datasets(Dinerstein et al.==

292 ==2017)== Furthermore, ~~In their study, Singh et al. (2020) classify drought coping strategies of forest and ecosystems~~

293 ~~under changes to their hydroclimate – which are not apparent from just precipitation and tree cover data, but~~

294 ~~also highlight (and validate) thresholds beyond which forest savanna transitions occur.~~ These adaptation

295 dynamics ~~thus,~~ align with the alternative stable state theory (i.e., forest's stabilising feedback under

296 hydroclimatic changes and tipping risk beyond certain hydroclimatic extremes) (Hirota et al., 2011), which

297 makes S_r more representative of the transient state of the ecosystem than precipitation (Singh et al., 2022).

298 ~~Due to their strong influence over hydroclimate and ecological systems (Tumber Dávila et al., 2022; Wang-~~

299 ~~Erlandsson et al., 2022), we use~~ We, thus, use these mass-balance derived S_r thresholds to project rainforest

300 transitions and tipping risk under future climate change. A detailed description of how previous studies have

301 projected rainforest tipping (~~Supplementary~~ Table S3), and how S_r-based framework builds upon their

302 shortcomings is mentioned in Supplementary ~~description~~Information.

303

2.3.2 2.3.3 Projecting forest transitions under future climate change

305 ~~Some previous studies have directly used the ensemble of hydroclimatic estimates to analyse tipping (Staal et~~

306 ~~al., 2020; Salazar et al., 2007). However, ESMs simulate Earth system processes based on their unique~~

307 ~~parametrisations and biases. Since an ensemble aggregates hydroclimatic estimates from different ESMs, it~~

308 ~~generalises the understanding of Earth system processes between different ESMs (Baker et al., 2021;~~

309 ~~McFarlane, 2011; Yuan et al., 2022). Therefore, we qualitatively assessed (i.e., by classifying) the ecosystem's~~

310 ~~water stressed state using S_r (Singh et al., 2020) for each ESM individually.~~ To project forest transitions under

311 future climate ~~For this~~, we ~~have to follow~~ first ~~three steps: (i) calculating~~ classify forests based on S_r thresholds

312 under the current and future climate ~~and classifying terrestrial ecosystems based on S_r thresholds~~. Based on

313 this classification, we ~~(ii) calculating S_r under future climate and using S_r thresholds to classify terrestrial~~

314 ~~ecosystems in the future, and (iii)~~ analys~~ing~~ potential transition for each ESM and aggregate the results ~~using~~

315 ~~current and future ecosystem classification~~ (Fig. 1). We start by classifying forests under current climate

316 following the approach by Singh et al. (2020), which uses the

317 ~~First, using a mass-balance approach, we determine the maximum annual accumulated water deficit~~

318 ~~from~~ (empirical) daily estimates of CHIRPS precipitation and ensemble evaporation ~~(over several years (~~2001-

319 2012~~, in this case)~~ ~~(see Supplementary Methods~~Appendix A1 and Sect. 2.3.2) ~~(.~~ ~~We then use a 20-year drought~~

320 ~~return period based on Gumbel extreme value distribution to simulate S_r under the current climate. Thus, S_r~~

321 ~~refers to the maximum deficit expected to occur every twenty years under static climate conditions. We~~

322 ~~acknowledge that grasslands and savanna adapt to shorter drought return periods (i.e., <10 years and 10-20~~

323 ~~years, respectively). In contrast, forests adapt to long drought return periods (>40 years) (Wang-Erlandsson et~~

324 ~~al., 2016). However, to avoid artificially introduced S_r transitions between landscapes, we chose a uniform 20-~~

325 ~~year drought return period (following Bouaziz et al., 2020; Nijzink et al., 2016), rather than assigning different~~

326 ~~drought return periods to different land cover types (i.e., forest, savanna and grassland) (Singh et al., 2020).~~

327 ~~In this study, we use Singh et al. (2020) S_r based classification scheme, which classifies terrestrial ecosystems as~~

328 ~~lowly water stressed, moderately water stressed, highly water stressed forests and savanna grassland regime.~~

329 ~~This classification is based on empirically observed patterns in the ecosystem's above- and below-ground~~

330 structure (i.e., the statistical relationship between tree cover and S_r), hydrology, and hydroclimate; and

331 validated against empirical rooting depth (Fan et al., 2017) and ecoregion datasets(Dinerstein et al., 2017).

332 Here, lowly, moderately and highly correspond to the state of the forest under different levels of water stress

333 (i.e., quantifying the magnitude and duration of water-deficit experienced by vegetation which can inhibit plant

334 growth. We directly used the S_r-based thresholds estimated by Singh et al. (2020) for ecosystem classification

335 under current climate conditions (detailed description in Table 1 of Singh et al., 2020) (Fig. 1a). Since we are

336 only interested in forest transitions, It should be noted that the the savanna-grassland ecosystems classified as

337 savanna under the current climate are excluded from this analysis. For South America, these empirical S_r

338 thresholds are ≤100 mm (for lowly; also referred to as 'lower S_r threshold'), 100-400 mm (for moderately) and

339 >400 mm (for highly water-stressed forests; also referred to as 'upper S_r threshold') (Fig. 1a). For Africa, these

340 S_r thresholds are ≤100 mm (for lowly), 100-350 mm (for moderately) and >350 mm (for highly water-stressed

341 forests). Higher S_r implies a need for larger storage to buffer water deficit, which previous studies found

342 corresponds to plants expanding their roots vertically and laterally to maximise storage (Singh et al., 2020). The

343 difference in S_r thresholds between both continents is due to the presence of water-use efficient C4 grasses in

344 Africa, which reduces the competitiveness for moisture uptake between tree species and grasses – leading to a

345 lesser need for root zone storage in the ecosystem(Singh et al., 2020).

346 SecondNext, for determining classifying ecosystems under future S_r climate scenarios, we follow the

347 same mass-balance approach as empirical ((see Supplementary MethodsAppendix A1)). However, as

348 mentioned previously, since different precipitation and evaporation estimates from ESMs do not align are based

349 on different research groups' understandings of Earth system processes and are therefore parametrised

350 differentlywith empirical estimates (Baker et al., 2021; McFarlane, 2011), we employ a bias-correction method.

351 Specifically, we . Therefore, it does not make sense to directly use the empirical (2001-2012) S_r thresholds

352 obtained under current climate conditions to classify S_r from future CMIP6 ESMs simulations. Furthermore,

353 since daily estimates of precipitation and evaporation are not publicly available for all CMIP6 ESM simulations,

354 it would not be logical to directly compare them with monthly precipitation and evaporation derived S_r

355 (Supplementary Method and Supplementary Fig. 8). To resolve this, we used the a histogram equivalence

356 method (Piani et al., 2010) to adjust empirical S_r thresholds to comparable CMIP6 S_r thresholds for various ESMs

357 (Table S1) (i.e., a bias-correction method). This involves, first, calculating S_r using CMIP6-historical precipitation

358 and evaporation estimates between 2000-2014 (Appendix A1 and Fig. S8). Here, the We then determine a

359 percentile-equivalent S_r thresholds for the empirical S_r thresholds is calculated individually for each of the thirty-

360 three CMIP6-ESMs under the current climate (CMIP6-historical between 2000-2014). For exampleexample, if

361 an empirical S_r of 100 mm corresponds to the 10th percentile (n = 20% of total pixels), in the empirically-derived

362 S_r sample (n = 20% of total pixels), we find the 10th percentile equivalent in the CMIP6-historically-derived S_r-S_r,

363 which may is considered its equivalent, but this can be higher or lower than 100 mm for each ESM (Fig. 1 and

12

Formatted: Font: Italic
Formatted: Subscript
Formatted: Font: Italic
Formatted: Subscript

364 Supplementary Table S1). These percentile-equivalent S_r thresholds are then used to classify ecosystems both
365 under current (CMIP6-hsitorical; 2000-2014) and future climate (CMIP6-SSPs; 2086-2100)

366 Percentile equivalent S_r thresholds are calculated for all ESMs individually under current climate
367 conditions (i.e., using CMIP6-historical estimates between 2000-2014) (Fig. 1b). Classifying savanna under
368 future climate requires an additional step as outlined in Appendix A3. These histograms analysed thresholds are
369 referred to as percentile-equivalent lower and upper S_r thresholds. To classify ecosystems under future climate
370 (2086-2100), we directly overlay the CMIP6 historical (2000-2014) percentile equivalent lower and upper S_r
371 thresholds to CMIP6-SSP derived S_r (2086-2100) (Fig. 1b and Supplementary Table 1). For our analysis, we chose
372 the same period of 15 years for both CMIP6-historical (2000-2014) and CMIP6-SSP (2086-2100) hydroclimate,
373 representing the epoch of current and future climate. Furthermore, the time-period for CMIP6-historical (2000-
374 2014) is chosen such that it will be close to the simulation period of empirical S_r (i.e., 2001-2012).

375 Under future climate change, some ecosystems will remain forest, while others will transition to savanna.
376 However, despite the analysis above capturing the change in S_r, it is difficult to discern whether an ecosystem
377 is a forest or savanna just with S_r (the above analysis only classifies ecosystems as forests). Savanna and
378 grassland ecosystems experience considerably less precipitation than forests and can show high precipitation
379 seasonality. However, because they also have lower evaporation than forests, their accumulated deficit and,
380 therefore, S_r is also less(Singh et al., 2020). These low S_r patterns might conceal savannas as a lowly or
381 moderately water stressed forests (since these forests also have low water deficit and therefore lower S_r)
382 (Supplementary Fig. 4a). Segregating them is easier under the current climate, where we have several remote
383 sensing products capturing vegetation structure (e.g., tree cover, tree height, floristic patterns)(Hirota et al.,
384 2011; Aleman et al., 2020; Xu et al., 2016). However, under future climate, we must find a proxy. Previous
385 studies have either depended on some vegetation structure metric derived from the models themselves (e.g.,
386 the fraction of forest cover or net primary productivity)(Jones et al., 2009; Boulton et al., 2013), or had assumed
387 that no other vegetation would replace forests. Therefore, the latter assumption assesses the possible extent
388 of forest ecosystems under future hydroclimatic changes(Staal et al., 2020). Since ESMs use IAM-derived land-
389 use scenarios solely based on macro-socioeconomic factors(Ma et al., 2020), and not biophysical processes, the
390 ecosystems are not in equilibrium with their climate. We went with the latter assumption of assessing the
391 theoretically possible extent of forest ecosystems under hydroclimatic changes (i.e., the ecosystem is in
392 equilibrium with their climate).

393 We did this using mean annual precipitation and the precipitation seasonality index range obtained under
394 the current climate (2001-2012) for forest classes (i.e., lowly, moderately, and highly water-stressed forest) and
395 savanna-grassland regime (Supplementary Fig. 4). The ecosystems (i.e., grid cells) falling outside the range of
396 bias-corrected mean annual precipitation and precipitation seasonality index of forest classes are classified as
397 'savanna' (this includes grassland). This way, not only do we segregate forests and savanna ecosystems under

Formatted: Font: Italic
Formatted: Subscript

ThirdUltimately, we evaluate potential transitions by comparing ecosystems classified under current climate conditions (*this excludes savanna*) with those under future climate conditions (*this includes savanna*) (Sect. 2.3.2). These transitions are divided into three distinct categories This classification allows us to evaluate tree types of transitions (Fig. 1c and Fig. A2):

i. **Forest-savanna transition:** This refers to current climate forest ecosystems that risk transitioning to a savanna under future climate change(i) current forest ecosystems that will transition to savanna in the future — referred to as forest-savanna transition,.

ii. **Transition to a more water-limited state:** This includes ecosystems that shift to a higher water-limited state in the future. For example, if a forest currently classified as lowly water-limited transitions to either a moderately or highly water-limited state in the future, it would fall under this category.

iii. (ii) forest ecosystems that become 'more' water-stressed in the future, and **Reversion to a less water-limited state:** (iii)This includes ecosystems that shift to a lower water-limited state in the future.forest ecosystems that become 'less' water-stressed in the future. For example, a lowly water-stressed forest transitioning to a moderately or highly water-stressed forest is considered as a 'transition to a more water-stressed state'. Whereas a transition from highly to a moderately or lowly water-stressed forest is considered a 'transition to a less water-stressed state'. We synthesise the results from all CMIP6 ESMs under different SSP scenarios (Fig. 1).

HereTo aggregate the results from all ESMs, grid cells with > 50% of model convergence are referred to as 'moderate-high model agreement', 20-50% as 'moderate model agreement' and ≤ 20% as 'low model agreement'. In the Results section, we primarily discuss estimates from scenarios >20% and >50% model convergence. While a threshold of >20% may seem low given the total number of ESMs analysed, it is important to recognise the variable and often limited capabilities of these ESMs, particularly in simulating biophysical

14

interaction and emerging properties due to our limited understanding of the Earth system (Lenton et al., 2019; Stevens and Bony, 2013)~~(Arora et al., 2023; Reyer et al., 2015)~~. Opting for a majority-based consensus in ESMs could overlook critical tipping risks identified by a minority of models, which might provide insights as valid as those from more widely agreeing models (Arora et al., 2023; Reyer et al., 2015).

~~However, this methodology has two major assumptions: (i) We assume that the empirically derived S_r thresholds remain valid in the future, and (ii) ESM projected hydroclimatic estimates represent the actual climate (this includes the influence of atmospheric moisture flows on hydroclimate). To address the uncertainty due to the former case, we do several sensitivity analyses to check its influence on potential transitions. Whereas in the latter, we explicitly apply this methodology across a wide range of available ESMs under four SSP scenarios to highlight the agreements and conflicts between the end results. The implications of both these assumptions are discussed in the Discussion sub-section 'Limitation and sensitivity analyses'. Furthermore, the discrepancies between the prescribed land use and our methodology-derived transitions are discussed in Fig. 5.~~

2.4   Sensitivity analyses

Our ~~However, this~~ methodology ~~has~~operates under two ~~major~~key assumptions: (i) ~~We assume that~~ the empirically derived S_r thresholds remain valid in the future~~,~~ modifying their critical thresholds (Doughty et al., 2023), and (ii) ~~ESM projected~~the hydroclimatic estimates projected by ESMs accurately represent the actual climate, even though~~ ~~ these models have prescribed land-cover (Hurtt et al., 2020)~~(this includes the influence of atmospheric moisture flows on hydroclimate)~~. To address the uncertaint~~y~~ies related ~~y due~~ to the ~~former~~first assumption~~case~~, we ~~do~~conduct ~~several~~four sensitivity analyses to ~~check~~assess the robustness ~~its influence~~ of our analysis~~on potential transitions.~~: (a) assuming that the regions exceeding the 99th percentile S_r are prone to a forest-savanna transition, as high S_r investment could be unrealistic from the perspective of plants under future climate change, (b) evaluating forest transitions using three different evaporation datasets, (c) assessing forest transitions under 10- and 40-year drought return periods, and (d) adjusting the forest-savanna transition thresholds.

~~Whereas~~Regarding ~~in the latter~~second assumption, we explicitly apply this methodology across a wide range of available ESMs under four SSP scenarios to ~~highlight the~~identify ~~agreements~~consistencies and ~~conflicts~~discrepancies ~~between~~in the results. Additionally, the discrepancies between the prescribed land-use and the forest transitions derived from our methodology, as well as t~~The~~ implications of ~~both~~these assumptions are ~~discussed~~detailed in the Discussion section~~ sub-section 'Limitation and sensitivity analyses'. Furthermore, the discrepancies between the prescribed land-use and our methodology-derived transitions are discussed in Fig. 5.~~

465 ~~Since our study relies on ecosystem classification thresholds based on S_r, to evaluate the robustness of our~~
466 ~~analysis, we conducted four sensitivity analyses: (i) by assuming that the regions that exceed the 99th percentile~~
467 ~~S_r are prone to a forest-savanna transition as high S_r investment could be unrealistic from the perspective of~~
468 ~~plants, (ii) evaluating forest transitions individually for all three evaporation datasets, (iii) evaluating forest~~
469 ~~transitions under 10- and 40-year drought return periods and (iv) by changing the forest savanna transition~~
470 ~~thresholds.~~

3 Results

473 ~~In this study, we focus on three specific transitions: (i) Forest-savanna transition, (ii) forests' transition to a more~~
474 ~~water-stressed state, and (iii) reversion to a less water-stressed state (Fig. 2a).~~ We find that under future climate
475 conditions (2086-2100), considering >50% models' agreement, about one-fourth of the forests in both South
476 America and Africa are projected to transition (Fig. 2b-g). With >20% models' agreement, these transitions are
477 projected to occur for about three-fourths of the forests for both continents. Considering a lower threshold for
478 models' agreement causes double or triple counting of some transitions (Fig. 2b-g). To minimise this in further
479 analyses, we only consider >50% models' agreement for forests that transition to a more and less ~~water-~~
480 ~~stressed~~water-limited state. Furthermore, because (abrupt) forest-savanna transitions are under-represented
481 in ESMs (Drijfhout et al., 2015; Lenton, 2011; Maslin and Austin, 2012; Valdes, 2011), we consider >20% models'
482 agreement for them. Considering this, we not only reduce the overlap to <0.4% of the total forest area
483 (~~Supplementary~~ Fig. S9), but we also maximise highlighting forest-savanna transition risk for both continents.

484 We find that the risk of forest-savanna transitions mainly occurs in the Guiana Shield of South America,
485 and the southern and south-eastern regions of Africa (Fig. 3). Compared to Africa, forest-savanna transitions
486 are more prominent in South America under warmer climates (i.e., higher SSPs; Fig. 2b and 3). Our analysis
487 reveals that the extent of forest-savanna transitions in South America decreases from almost 1.32×10^6 km^2
488 (16.3% of total forest area in South America) under the highest emission scenario to 0.04×10^6 km^2 (0.5%) under
489 the lowest emission scenario (Fig. 2b). Interestingly, for Africa, the extent of forest-savanna transition did not
490 change much for different SSPs, i.e., (median) 0.25×10^6 km^2 with a maximum deviation of $\pm0.11 \times 10^6$ km^2
491 (minimum and maximum extent of transition between 3-6.6% of total forest area in Africa) (Fig. 2c).

492 When comparing the changes in forest-savanna transition risk areas relative to their immediate lower
493 warming scenarios, we find considerable increases for South America. The highest relative growth of
494 approximately 5.75 times is observed between SSP1 and SSP2, with the forest area under risk increasing from
495 0.04×10^6 km^2 to 0.23×10^6 km^2, respectively. It increases by 3.48 times from SSP2 to SSP3 (0.23×10^6 km^2 to
496 0.80×10^6 km^2), and by 1.65 times from SSP3 to SSP5 (0.80×10^6 km^2 to 1.32×10^6 km^2). For Africa, however,
497 the increases are more modest: the risk grows by 1.29 times from SSP1 to SSP2 (0.17×10^6 km^2 to 0.22×10^6

Formatted: English (United Kingdom)
Formatted: English (United Kingdom)
Formatted: English (United Kingdom)
Formatted: English (United Kingdom)
Formatted: English (United Kingdom)
Formatted: English (United Kingdom)
Formatted: English (United Kingdom)
Formatted: English (United Kingdom)
Formatted: English (United Kingdom)

498 km²), by 1.63 times from SSP2 to SSP3 (0.22 × 10⁶ km² to 0.36 × 10⁶ km²), and is observed to decrease by 0.72
499 times from SSP3 to SSP5 (0.36 × 10⁶ km² to 0.26 × 10⁶ km²).

500 By evaluating changes to their hydroclimate, we find that under warmer climates, forest-savanna
501 transition regions in both continents are projected to experience a decrease in precipitation. Furthermore, we
502 observe an increase in precipitation seasonality for South America, whereas Africa shows a decrease
503 (~~Supplementary~~ Fig. S12). Here, an increase in precipitation seasonality (seasonal variability in precipitation
504 over the year) creates ~~stress~~water-limited conditions for the ecosystem. In contrast, a decrease in seasonality
505 and precipitation in Africa corresponds to a lower moisture availability altogether. Nevertheless, for both these
506 continents, this transition seems to occur for the previously highly ~~water-stressed~~water-limited forests under
507 the current climate, followed by moderately, with the least contribution from lowly ~~water-stressed~~water-
508 limited forests (Fig. 3). This highlights the looming risk on highly ~~water-stressed~~water-limited forests to
509 experience a forest-savanna transition under warmer climates.

510 Forests that transition to a 'more' ~~water-stressed~~water-limited state in South America are spatially
511 aggregated towards the border between Brazil, Colombia, and Peru – covering a considerable portion of the
512 Central Amazon (Fig. 3). Whereas for Africa, these forests exist in moderate to small patches towards the
513 northern and southern extent of central Congo rainforests. We observe that these transitions account for most
514 of the projected changes to forests' states across both continents (Fig. 2d,e), with the transition to just the
515 'highly ~~water-stressed~~water-limited forest' accounting for more than three-fourths of all such transitions (Fig.
516 3). We observe that South American forests gradually become increasingly ~~water-stressed~~water-limited under
517 warmer climates, with maximum and minimum projected transition of 1.89 × 10⁶ km² (23.4%) and 1.61 × 10⁶
518 km² (19.9%) observed under the highest and lowest emission scenarios, respectively (Fig. 2d,e). Whereas for
519 Africa, the change in the ~~water-stressed~~water-limited state of the forests under different SSP scenarios remains
520 almost similar (i.e., median 1.14 (±0.06) × 10⁶ km²; 19.6-22.2%). Analysis of their hydroclimatic changes reveals
521 that water-~~stress~~limitation is induced by both a decrease in precipitation and an increase in seasonality in South
522 America (~~Supplementary~~ Fig. S13). In contrast, water-~~stress~~limitation in Africa is driven solely by an increase in
523 seasonality. We observe that these newly ~~water-stressed~~water-limited forests seem to have permeated to
524 regions that were previously (under the current climate) dominated by lowly and moderately ~~water-
525 stressed~~water-limited forests (Fig. 3). Here, this shift only signifies the changes to hydroclimatic conditions
526 allowing forests to transition to a more ~~water-stressed~~water-limited state, rather than the changes to the
527 floristic composition of terrestrial species from one location to another. Although such a shift under changing
528 climate is not unlikely (Esquivel-Muelbert et al., 2019), they are not analysed in this study.

529 Forests that revert to a 'less' ~~water-stressed~~water-limited state in South America are primarily observed
530 in the south-eastern Amazon, with small patches observed towards eastern Brazil and the western coast of
531 Equatorial Guinea and Gabon (Fig. 3). For Africa, the reverted forests exist in patches in the northern and

532 southern regions of the Congo rainforest. Furthermore, for South America, we observe a gradual decrease in
533 these reversions with an increase in warming. Here, we observe the lowest reversion of 0.23×10^6 km^2 (2.8%)
534 under the highest emission scenario and the highest reversion of 0.67×10^6 km^2 (8.4%) under the lowest
535 emission scenario (Fig. 2f,g). For Africa, these trends remain almost similar under all SSPs (i.e., median 0.18
536 ($\pm$0.05) $\times 10^6$ km^2; 2.2-3.5%). Comparing these transitions with their hydroclimatic changes reveals an overall
537 increase in precipitation (~~Supplementary~~ Fig. S14). Interestingly, we observe a much higher precipitation
538 increase for South America under high-emission scenarios than those in lower-emission scenarios. However,
539 we find that precipitation seasonality is also higher for these ecosystems under warmer climates (Fig. S14). This
540 suggests that increased precipitation without changes to precipitation seasonality helps decrease the water-
541 ~~stress~~ limitation of the ecosystem, compared to the ecosystems that experienced a simultaneous increase in
542 both.
543 Our sensitivity analysis, detailed in Appendix B1, reveals a consistent pattern of forest transitions across
544 various scenarios.
545
546
547
548
549
550

18
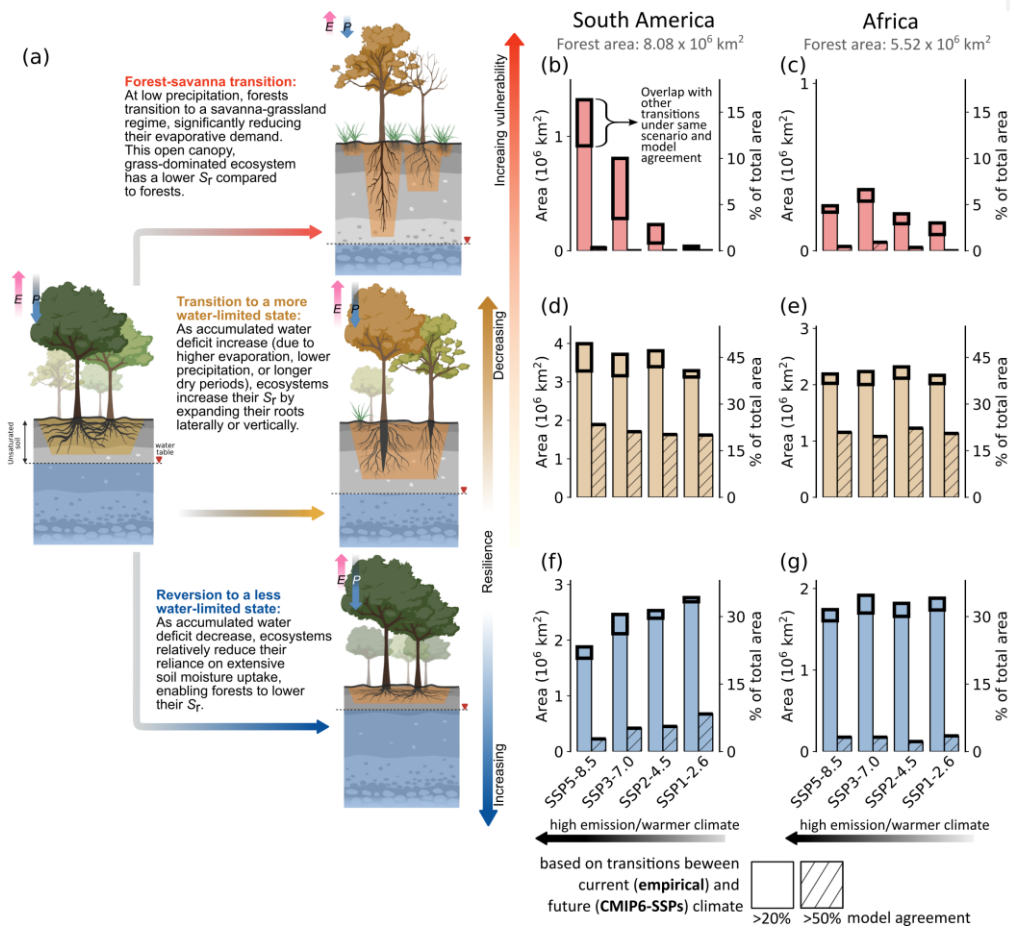
Figure 2: Comparing the potential transitions under different SSP scenarios. (a) The state of the ecosystem, both above- and below-ground, (post-transition) under future climate, quantifying **(b,c)** forest-savanna transition, **(d,e)** forests' that transition to a more ~~water-stressed~~water-limited state and **(f,g)** revert to a less ~~water-stressed~~water-limited state for South America and Africa (present forest area mentioned on the top of (b,c)), respectively. For the analysis above, transitions are calculated for grid cells with model agreement >20% (plain bar plot) and >50% (hatched bar plot). These quantifications show changes in the forest area based on ecosystem transitions under empirical-current (2001-2012) and future (2086-2100) climate conditions. For all these transitions, we assume that the hydroclimate and vegetation are in equilibrium. Analyses comparing ecosystem transitions based on CMIP6-historical (2000-2014) and future (2086-2100) climate conditions are shown in ~~Supplementary~~ Figs. S10 and S11. For each transition, the total area of spatial overlap with other transitions under the same SSP scenario and model agreement is highlighted with thick black bars. The P and E arrows in (a) describe the relative magnitude of precipitation and evaporation fluxes. The illustration in (a) is adapted from Singh et al. (2020) and created with BioRender.com.

566
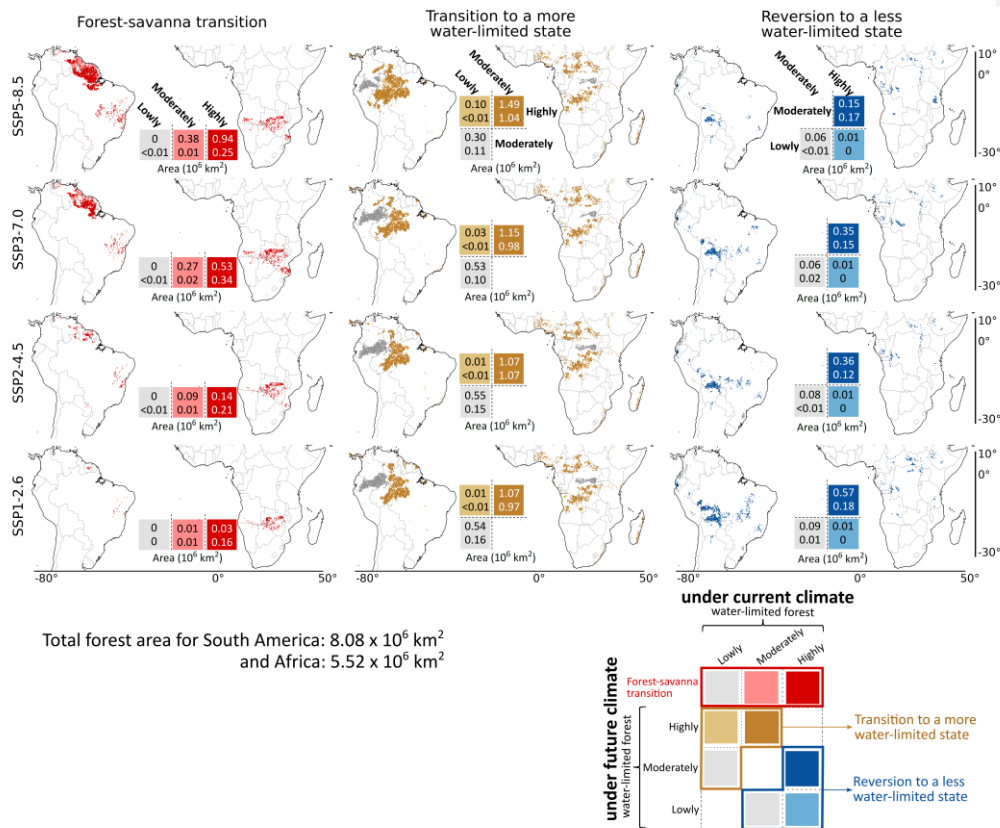
Figure 3: Spatial extent of potential transitions with respect to their current state under different SSP scenarios. We analysed transitions, explicitly focusing on forest-savanna transition, transition to a more ~~water-stressed~~water-limited state, and reversion to a less ~~water-stressed~~water-limited state, by comparing different ecosystem classes under current (empirical; 2001-2012) and future (SSPs; 2086-2100) climate conditions (as defined in Fig. 2). All transitions shown above are analysed for moderate-high (>50%) model agreement, except forest-savanna transition, for which moderate (>20%) model agreement is considered. Values overlaying the legends correspond to the total area of transition for South America (top values) and Africa (bottom values).

574

4   Discussion

4.1   Asynchronous resilience risks under future climate change

Our analysis reveals the spatial extent of potential ecosystem transitions in South America and Africa and their vulnerability to future climate change (Fig. 2 and 4). For South America, we find a clear indication of a decrease in forest resilience (i.e., an increase in ~~water-stressed~~water-limited forests) and an increase in forest-savanna transition risk under warmer climates (Fig. 2b,d,f). In contrast, these trends are not symmetric for Africa, where

20

581 transition risk shows only slight variation across the different SSPs (Fig. 2c,e,g). Similar to the results of this

582 study, previous studies on rainforest tipping have also suggested that exceeding 1.5-2°C will considerably

583 increase the tipping risk (Flores et al., 2024; Jones et al., 2009; Parry et al., 2022), with the Guyana Shield in the

584 Amazon being the most susceptible under future climate change (Cox et al., 2004; Staal et al., 2020) (Fig. 3 and

585 ~~Supplementary~~ Table S3). Previous studies also agree that, in contrast to the Amazon, the projected risk to

586 Congo rainforests is not substantial (Higgins and Scheiter, 2012; Staal et al., 2020) (Fig. 2). Despite it being

587 unclear to what extent the ESMs represent the correct carbon-water dynamics (Koch et al., 2021), our results

588 show a further divergence between Amazon's and Congo's responses to different SSPs (Fig. 2 and

589 ~~Supplementary~~ Figs. S12-S14). This could either be caused simply by a different response to changes in

590 precipitation patterns over the respective regions (Kooperman et al., 2018; Li et al., 2022) or a different

591 response to increased CO_2 levels in the atmosphere (Brienen et al., 2015; Hubau et al., 2020; Trumbore et al.,

592 2015).

593 Previous empirical studies have linked these divergent responses to evolutionary and biogeographical

594 differences between the ecosystems, which resulted in distinct species pools that uniquely influence each

595 ecosystem's adaptability and response to climate change (Fleischer et al., 2019; Hahm et al., 2019; Hubau et

596 al., 2020; Slik et al., 2018). These studies found that forest ecosystems in the Amazon ~~are~~ tend to be more

597 dynamic – grow faster due to high CO_2 levels in the atmosphere – than those in the Congo rainforests. However,

598 these fast-growing trees also die young due to them investing substantially less in their adaptive strategies

599 against perturbations than (less dynamic) old-growth forests (Brienen et al., 2015; Körner, 2017; Rammig,

600 2020). This makes the Amazon rainforest especially sensitive to CO_2 emissions pathways, as ~~For these~~

601 ~~ecosystems,~~ the positive influence of CO_2 fertilisation-induced growth is counteracted by the negative impact

602 of warming and droughts, thereby ~~making the Amazon rainforest especially sensitive to CO_2 emissions~~

603 ~~pathways, which can~~ exacerbating the risk of~~e~~ forest mortality under high emission scenarios (Brienen et al.,

604 2015; Hubau et al., 2020; Yang et al., 2018). In this case, the projected changes to the future hydroclimate could

605 be an artefact of decreased transpiration and precipitation due to forest mortality, rendering the rainforests

606 vulnerable to tipping. ~~be due to evolutionary biogeographical differences in the ecosystems leading to divergent~~

607 ~~species pools and resulting differences in ecosystems' functional attributes (Hubau et al., 2020; Singh et al.,~~

608 ~~2020; Slik et al., 2018), and nutrient limitation (Fleischer et al., 2019).~~In contrast, terrestrial species in Congo

609 rainforests appear more resilient, having adapted to severe droughts during glacial periods, which makes them

610 better equipped to handle episodic water-induced perturbations than Amazon (Cole et al., 2014). ~~In this case,~~

611 ~~the projected changes to the future hydroclimate could be an artefact of forest mortality decreasing~~

612 ~~transpiration and precipitation over the rainforest. be due to evolutionary biogeographical differences in the~~

613 ~~ecosystems leading to divergent species pools and resulting differences in ecosystems' functional attributes~~

614 ~~(Hubau et al., 2020; Singh et al., 2020; Slik et al., 2018), and nutrient limitation (Fleischer et al., 2019).~~

Formatted: Swedish (Sweden)

Field Code Changed

Formatted: Swedish (Sweden)

615 ~~This, combined with accelerated warming and frequent droughts faced by Amazon in recent decades,~~
616 ~~has made them more vulnerable to climate change than the Congo rainforests (Yang et al., 2018). For these~~
617 ~~ecosystems, the positive influence of CO_2 fertilisation-induced growth is counteracted by the negative impact~~
618 ~~of warming and droughts – thereby making the Amazon rainforest especially sensitive to CO_2 emissions~~
619 ~~pathways, which can exacerbate forest mortality under high emission scenarios (Brienen et al., 2015; Hubau et~~
620 ~~al., 2020). In this case, the projected changes to the future hydroclimate could be an artefact of forest mortality~~
621 ~~decreasing transpiration and precipitation over the rainforest.~~ ~~Previous studies also hint that these~~
622 ~~asynchronous resilience risks in the rainforest could~~ ~~be due to evolutionary biogeographical differences in the~~
623 ~~ecosystems leading to divergent species pools and resulting differences in ecosystems' functional attributes~~
624 ~~(Hubau et al., 2020; Singh et al., 2020; Slik et al., 2018), and nutrient limitation (Fleischer et al., 2019). According~~
625 ~~to them, the terrestrial species in Congo rainforests have already experienced severe droughts in the glacial~~
626 ~~periods, which makes them more adaptive to episodic water-induced perturbations than Amazon (Cole et al.,~~
627 ~~2014).~~ Nevertheless, with compounding influence from land-use and climate-induced hydroclimatic changes
628 (Davidson et al., 2012), these rainforests risk tipping to a savanna state. Our results highlight that by keeping
629 the mean global surface temperature below 1.5-2°C warming (which in this case is equivalent to SSP1-2.6
630 relative to the pre-industrial), we minimise forest-savanna transition risk and maximise recovery – thereby
631 improving the resilience of rainforest ecosystems (Fig. 2, 3 and 4).

632

633 ~~**4.2 Inferring adaptations from root zone storage capacity**~~

634 ~~We analyse S_r to relate changes in precipitation, precipitation seasonality and atmospheric water demand (Figs.~~
635 ~~1-2 and Supplementary Figs. 12-14) with the ecosystem's dynamic subsoil adaptation (Singh et al., 2020). Here,~~
636 ~~the observed transitions are the aftermath of the ecosystem's minimising and (as observed in most cases)~~
637 ~~maximising their subsoil storage capacity to offset water-deficit and efficiently utilise available subsoil moisture~~
638 ~~under future climate change (Fig. 2a). Since plants prefer moisture uptake from the shortest pathway with the~~
639 ~~least resistance, a decrease in water deficit – increase in precipitation, decrease in seasonality and atmospheric~~
640 ~~water demand – will enhance the availability of moisture at shallow depths and motivate vegetation to utilise~~
641 ~~shallow roots for moisture uptake (Bruno et al., 2006). This allows the forests to reduce their total subsoil~~
642 ~~storage capacity while transitioning towards a less water-stressed state (Singh et al., 2020; Bruno et al., 2006).~~
643 ~~However, an increase in water deficit forces forest ecosystems to invest in their subsoil structure and~~
644 ~~adapt strategies to store surplus moisture from wet seasons to ensure their survival during dry seasons,~~
645 ~~meaning that ecosystems transition to a more water-stressed state (Singh et al., 2020). Furthermore, higher~~
646 ~~investment in deeper and extensive lateral roots exposes plants to embolism-related hydraulic failures (Liu et~~
647 ~~al., 2022), thus increasing forest mortality risk under droughts (Aleixo et al., 2019; Anderegg et al., 2016;~~
648 ~~Bittencourt et al., 2020). This, along with other biotic and abiotic factors, including the maximum rooting extent~~

22

649 ~~of individual tree species (Canadell et al., 1996; Jackson et al., 1996), geological factors limiting roots to utilise~~
650 ~~deeper subsoil water and nutrient resources (Schenk and Jackson, 2002), and anaerobic conditions influencing~~
651 ~~microbial population at deeper depth (Dittert et al., 2006), among others (Alvarez Uria and Körner, 2007;~~
652 ~~Brunner et al., 2015); caps the maximum adaptive capacity of the ecosystems to invest(Singh et al., 2020) and~~
653 ~~may influence diverse adaptive behaviour between ecosystems (Bonal et al., 2016). Under further episodic~~
654 ~~changes in soil moisture availability, i.e., beyond their maximum adaptive capacity, ecosystems survive by~~
655 ~~adapting to a new regime with relatively low moisture demand and more drought tolerance (Sankaran, 2019),~~
656 ~~which in this case is similar to a savanna ecosystem (Singh et al., 2020, 2022a).~~

657

658 **4.~~3~~4.2 Changes in atmospheric moisture flow drive~~s~~ forest-savanna transition~~s~~**

659 Among all transitions, the most noticeable and catastrophic (since it is difficult to revert) is the forest-savanna
660 transition projected in the Amazon's Guiana Shield of South America, and over the southern and south-eastern
661 parts of Africa (Fig. 3 and 4). These transitions are associated with the shifting of the inter-tropical convergence
662 zone (ITCZ) (Mamalakis et al., 2021), which decreases precipitation and increases precipitation seasonality over
663 the continents. For South America, the creation of these low-pressure bands allows the trade winds to bring in
664 considerable moisture from the equatorial Atlantic Ocean over to Amazon by passing through the Guiana Shield
665 and ultimately carrying it across the La Plata Basin via the South American low-level jet (Bovolo et al., 2018; van
666 der Ent et al., 2010; Zemp et al., 2014). Similarly, for Africa, ~~where~~ south-eastern trade winds bring moisture
667 from the Indian Ocean over the centre of the African continent (Mamalakis et al., 2021).

668 Under a warmer climate, sea surface temperature over the equatorial Atlantic and the northern Indian
669 Ocean is projected to increase (Pascale et al., 2019; Zilli et al., 2019), leading to a southward shift in ITCZ over
670 the eastern Pacific and Atlantic Oceans, and northward over east Africa and the Indian Ocean (Mamalakis et al.,
671 2021; Xie et al., 2010). Previous studies also acknowledge that the intense surface warming over the Sahara
672 under future climate can also attract ITCZ northwards in Africa (Cook and Vizy, 2012; Dunning et al., 2018;
673 Mamalakis et al., 2021). Since these shifts in ITCZ can potentially both ~~counteract~~ mitigate and aggravate
674 (especially critical for highly ~~water-stressed~~water-limited forests) the impact of (accumulated) water-deficit on
675 the forest ecosystem, including those ~~impacted~~ caused by localised deforestation ~~(Leite-Filho et al., 2021;~~
676 ~~Schumacher et al., 2022; Staal et al., 2018; Wunderling et al., 2022).~~ (Leite-Filho et al., 2021; Schumacher et al.,
677 2022; Staal et al., 2018; Wunderling et al., 2022); ~~It~~ it warrants the need to include changes in atmospheric
678 circulation for studies analysing the impact of future climate on the resilience of ~~natural and human-~~
679 ~~influenced~~forest ecosystems (Staal et al., 2020; Zemp et al., 2017).

680

Formatted: Indent: First line: 0.5"
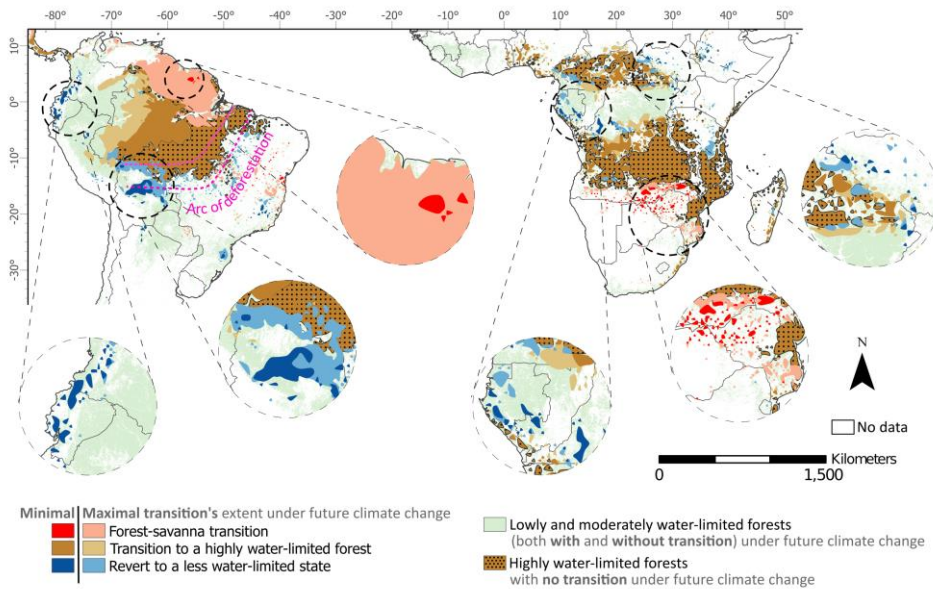
Figure 4: Minimal and maximal extent of potential ecosystem transitions under future climate change in the entire study region over South America and Africa. The three transition types are: forest-savanna transition, from any class to highly ~~water-stressed~~water-limited forests, and to a less water-~~stress~~limited state (see definitions in Fig. 2 and 3). For better visualisation of these transitions, in this figure, we first converted all grid cells to shape, merged them, and then smoothed them using the 'polynomial approximation with exponential kernel' function (with a tolerance value of 1) in ArcGIS pro. The unsmoothed version of the transitions is shown in Fig. 3. The minimal and maximal represent the minimum and maximum possible extent of transitions (as quantified in Fig. 3) based on changes between current (empirical; 2001-2012) and future (SSPs; 2086-2100) climate conditions regardless of the SSP scenarios.

4.4~~4.3Comparing~~ Discrepancy between prescribed future land-use ~~with~~ and projected transitions

~~Besides different radiative forcing, the~~The ~~CMIP6-ESMs also use prescribed~~ land-use information in CMIP6-ESMs is not biophysically simulated, but prescribed based on simulations from Integrated Assessment Models (IAMs) ~~scenarios~~ for each SSP scenario ~~(Hurtt et al., 2020).~~ (Hurtt et al., 2020). Therefore, it is ~~interesting~~ valuable to ~~check~~examine whether these prescribed land-use scenarios agree or conflict with the changes projected (assuming equilibrium between hydroclimate and the ecosystem) ~~from~~by our S_r-based ecosystem ~~(classification and)~~ transitions (Fig. 5 and ~~Supplementary~~ Fig. S15-~~18~~S17).

The most noticeable discrepancies are observed in South America, ~~Our analysis reveals that~~ where the extent of forest-savanna transitions is ~~often~~underestimated in prescribed land-use scenarios ~~–~~compared to those projected in this study (i.e., prescribed land-use predicts forests in the region whose hydroclimate can't support forest~~prescribed land use predicts less non forested areas~~; Fig. 4 and 5a). ~~Whereas~~Additionally, in

24

South America, our analysis highlights the potential of some forests reverting to a 'less water-limited state' in places where the prescribed land-use in the ESMs suggest non-forest landscape (Fig. 4 and 5c). forests that revert to a 'less water stressed state' the is overestimated in our analysis (i.e., our analysis projects more forested areas; Fig. 5c). This These discrepanciesy arise is because the prescribed land-use categories in CMIP6-ESMs are prescribed (simulated in Integrated Assessment Models (IAMs)) (Hurtt et al., 2020) and do not shift in response to hydroclimatic changes. It is important to note that wmacroeconomic processes drive land-use scenarios from IAMsthe end of the Despite our approach assuming equilibrium and overlooking the temporal dynamics of transitions, based on broad climate change pattern (Sect 4.2), Despiteingsewe believe it more accurately represents the ecohydrological state of the ecosystems.

However, these Also, the land-use scenarios used in the ESMs are assumed to evolve in time (as a function of macro-economic processes (Ma et al., 2020)), whereas our study does not account for the time required for transitions to unravel, and assumes an equilibrium between the 21st-century hydroclimate (i.e., 2086-2100) and the ecosystems. In ESMs, this prescribed land land-uses that does not dynamically respond to hydroclimatic changes could can introduce errors in subsequent biophysical processes simulated in ESMs (Ma et al., 2020), affecting the accuracy of projected transitions. For example, prescribing a region as a forest to a (projected) that would be savanna grassland region in the future ESM (e.g., Fig. 5a) will lead to the extraction of deeper subsoil moisture in ESMs, which (actual) grasslands ecosystems do not have the capacity to access access (Ahlström et al., 2017; Yu et al., 2022), (Ahlström et al., 2017; Yu et al., 2022). This will result in an overestimation of the ecosystem's evaporation, potentially altering precipitation patterns downwind and leading to inaccurate water budget assessments for these ecosystems. Consequently, causing erroneous projections of the ecosystem state. and, therefore, will lead to overestimation of the ecosystem's evaporation and associated precipitation downwind; therebyleading to an erroneous projection of the ecosystem state. These discrepancies underscore the urgent need for enhancements in the land surface components of ESMs, enabling dynamic simulations of vegetation-climate feedbacks. Such improvements would provide a more accurate representation of the ecohydrology of terrestrial ecosystems and their response to changing climate conditions.

By analysing potential transitions based on hydroclimate-derived S_*, we highlighted the inconsistencies in prescribed land-use solely based on IAMs (Fig. 5).

Formatted: English (United Kingdom)

Formatted: Left, Indent: First line: 0.5"

Formatted: Check spelling and grammar

Formatted: Left

25
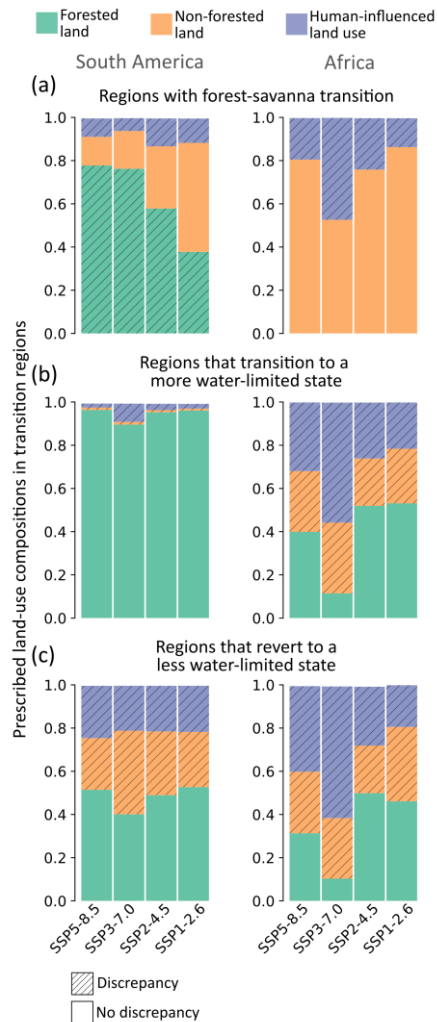
Figure 5: Prescribed land-use composition for each transition region under different SSP scenarios (median 2086-2100), calculated as the ratio between the prescribed land use area and the projected transition area. Regions where IAM prescribed land use are same as the projected transitions (from Fig. 3) are shown in plain colours (i.e., no discrepancy). Whereas regions where IAM-prescribed land use are differentdiffers from projected transitions are hatched (i.e., discrepancy).

4.54.4 Limitations and sensitivity analyses

This study assumesWe assume that the S_r-derived thresholds— used to classify terrestrial ecosystems under the current climate —conditions remain valid under future climate change. However, forests themselves are

742 dynamically adapting their structure and functions in response to climate change, altering their critical

743 thresholds (Doughty et al., 2023). Thus, assuming a static critical threshold~~in some cases, this~~ ~~might~~ may lead

744 to ~~an over- or under-estimation of~~ inaccuracies in estimating forests' ~~adaptability~~ resilience to future climate

745 change. For ~~example~~instance, under the CO_2 fertilisation effect, forests may become more water-use efficient

746 (i.e., ~~less~~ transpir~~e less~~ation and therefore need for a lower S_r) (Xue et al., 2015), potentially ~~, which will change~~

747 ~~the stability landscape in the future – implying a~~delaying their tipping under warming scenarios compared to ~~n~~

748 ~~underestimation of forest resilience~~ those projected in this study. Conversely, factors such as ~~Whereas~~ nutrient

749 limitation (Condit et al., 2013) or extensive human influence (van Nes et al., 2016) in the ecosystem~~s~~ might lead

750 to an earlier tipping than anticipated~~. – an overestimation of forest resilience~~.

751   However, the uncertainty surrounding the effect of CO_2 fertilisation, nutrient limitation, and human

752 influence on vegetation remain significant ~~makes them a~~ research frontier~~s~~ for ~~improving~~enhancing our

753 understanding of rainforest tipping ~~projections~~ under future climate change (Fleischer et al., 2019; Hofhansl et

754 al., 2016). ~~Furthermore~~Additionally, ~~local-scale~~ factors~~,~~ such as precipitation variability, species composition,

755 soil properties ~~and topography, might lead to a heterogeneous forest response (i.e., resilience) under~~, and

756 topography can contribute to varied local-scale forest responses to future climate change (Staal et al., 2020). It

757 should also be noted that though these uncertainties may hinder our understanding of local-scale forest

758 resilience, the influence of future hydroclimatic changes on forests ~~also~~ still constitutes major prediction

759 uncertainties. Therefore, in this study, regardless of how these influences are parametrised or simulated in each

760 ESM, we assume that hydroclimatic estimates projected by the ESMs represent the actual climate.

761   Of course, this assumption opens us ~~(~~and other studies projecting forest conditions~~)~~ ~~in the future~~ to

762 future climate change to certain limitations. ~~For example, o~~Our ~~capacity~~ability to project forest-savanna

763 transitions (or any transition) ~~depends~~relies on the model's ~~capability~~capacity to simulate complex feedbacks.

764 ~~On the one hand, s~~Some models ~~have a~~capture complex vegetation-atmosphere interaction~~,~~ – simulating local

765 and regional scale feedbacks across time (Ferreira et al., 2011; Jach et al., 2020)~~;~~. ~~On the other,~~ others ~~some~~

766 ~~models~~ reply ~~simulate these interactions based~~ on simpler parametrisation (Nof, 2008) (e.g., parametrisation

767 of ~~. Furthermore, some models might have a stronger~~ CO_2 fertilisation; ~~effect, whereas some weaker (~~Koch et

768 al., 2021). However, caution should be taken to not overgeneralise the functioning of tropical forests just from

769 the analysis presented in this study, and also realise the current potential of ESMs to simulate them (Staal et

770 al., 2020). We believe that ~~To address this, rather than using just one ESM,~~ ~~by~~ ~~we~~ consider~~ing~~ multiple

771 simulations from multiple ESMs under ~~multiple~~different SSP scenarios ~~(Fig. 2, Supplementary Figs. 5-6, and~~

772 ~~Supplementary Figs. 10-11). This way, we highlight not only the rainforest tipping risks, ,~~ not only do we ~~but~~

773 highlight ~~also~~ the agreements and conflicts between potential transitions; but also ~~that will~~ allow future studies

774 to disentangle vegetation-climate feedbacks and improve the modell~~ing of~~ed local-scale interactions (e.g.,

parametrisation of rooting/soil depth, ~~vegetation's water-uptake profile, species response to~~ CO$_2$ fertilisation) in the ESMs.

~~Moreover, since the projected transitions are sensitive to ecosystems' hydroclimatic changes and adaptive strategies, we perform sensitivity analyses on S_r (representing S_r based adaptation) and forest-savanna transition thresholds to check the robustness of the projected transitions (Figs. 1-2 and Supplementary Figs. 18-22). Fixing an extreme S_r threshold — signifying forest-savanna transition for ecosystems that cannot maintain their above-ground structure at high S_r — we observe some shifts close to the already projected risk regions and coastal regions (Fig. 3 and Supplementary Fig. 18). However, this transition risk in the coastal regions could be an artefact of interpolating hydroclimate estimates to higher resolution, and since oceans have more prevalent evaporation than land — it could lead to high S_r and, therefore, projection of tipping risk in coastal regions. We also discover that variations in the evaporation datasets and return periods utilized for calculating S_r have only a minimal effect on forest transitions (Supplementary Figs. 19-20). This is because, even though the forest classification thresholds may change due to different evaporation products under current climate (Singh et al., 2020), our histogram equivalence method ensures that forest classification under future climate adjusts relatively, resulting in minor alterations to the final outcome (Fig. 1b and Supplementary Figs. 19-20). Furthermore, while S_r values increase with increase in return periods, the impact of these changes is more noticeable for shorter return periods and less substantial for longer return periods (Wang-Erlandsson et al., 2016). Moreover, lowering the forest-savanna transition thresholds can lead to a reduction in forest-savanna transition risk due to an increase in precipitation range and seasonality for forest ecosystems (Supplementary Figs. 21-22). Despite these sensitivity analyses, the differences in transition magnitudes are minor, and the trends across different SSP scenarios for both continents remain similar (Fig. 2 and Supplementary Figs. 18-22). Therefore, the conclusions drawn from this study remain robust, even with variations in factors that could potentially affect forest transitions.~~

5 Conclusions

Classifying terrestrial ecosystems based on empirical and CMIP6 ESMs-derived S_r ~~— the ecosystem's capacity to store surplus moisture and access moisture during dry periods —~~ allowed us to assess the future transitions in the rainforest ecosystems. Our findings indicate that ~~The~~ climate under the lowest emission scenarios significantly ~~minimises~~ reduces the risk of rainforest tipping ~~risks~~ and maximises reversion to a less ~~water-stressed~~water-limited state~~s, whereas, while~~ ~~climate under the opposite is achieved in~~ the high emission scenarios have the opposite effect on the forest ecosystem. Specifically, ~~In~~ in the Amazon rainforest, the risk of forest-to-savanna transition ~~risks~~ increases ~~non-linearly~~considerably with ~~each degree of~~ incremental increase

in warming. Conversely, in the Congo, the variation in transition risk across different emission scenarios is relatively minor~~In contrast, the risk increase between different emission scenarios is not significant for Congo~~.

Notably, our analysis suggests ~~We believe that the results from this study can be used to further assess the direct and cascading influence of ecosystem transitions under future climate change on other natural and human influenced systems (e.g., the influence of rainforest tipping on downwind rainfall, agricultural production and global food supply chain). We find~~ very limited tipping risk that is 'unavoidable' (i.e., regions prone to a forest-savanna transition in all scenarios), and ~~whereas~~ the vast majority of potential transition risks can still be avoided by steering towards a less severe climate scenario, thereby ~~highlighting~~ underscoring the critical window of opportunity. ~~Furthermore~~Moreover, regions projected to ~~transition~~ revert to a less ~~water-stressed~~water-limited state ~~can~~ could potentially become more amenable to restoration and responsive to deforestation prevention efforts~~easier to restore and respond well to deforestation prevention measures~~. This study highlights the importance of restricting global temperature change below 1.5-2°C warming relative to the pre-industrial ~~global surface temperatures~~ levels to prevent ~~potential~~ forest ~~transition~~ tipping risks and provide the best conditions for effective ecosystem stewardship.

Appendix A: Methodology

A1. Root zone storage capacity calculation

Our method to calculate S_t is adopted from (Singh et al. (2020). For estimating S_t, we first obtained the water deficit (D_t) at daily time step from the daily estimates of precipitation (P_t) and evaporation (E_t) (Fig. A1) using:

$$D_t = E_t - P_t \qquad (A1)$$

Here, t denotes the day count since the start of the simulation, with simulation for each grid starting in the month with maximum precipitation. Second, we calculated the accumulated water deficit integrated at each one-day timestep for one year using:

$$D_{a(t+1)} = \max\{0, D_{a(t)} + D_{t+1}\} \qquad (A2)$$

Where $D_{a(t+1)}$ is the accumulated water deficit at each time step (Fig. A1). Here, an increase in the accumulated water deficit will occur when $E_t > P_t$, and a decrease when $E_t < P_t$. However, since this algorithm estimates a running estimate of root zone storage reservoir size, we use a maximum function to calculate the accumulated water deficit, which by definition can never be below zero. Not allowing $D_{a(t+1)}$ to be negative also means that excess moisture from precipitation will either contribute to deep drainage or runoff. Lastly, the

maximum accumulated annual water deficit ($D_{a,y}$) will represent the maximum storage required by the vegetation to respond to the critical dry periods (Fig. A1).

$$D_{a,y} = \max\{D_{a(t+1)}\} \quad t = 1:n-1 \tag{A3}$$

This simulation runs for a whole year, with n denoting the number of days in year y.

Although different terrestrial ecosystems (e.g., forest, savanna and grasslands) adapt to different drought return periods (de Boer-Euser et al., 2016; Gao et al., 2014; Wang-Erlandsson et al., 2016). For instance, grasslands and savanna adapt to shorter drought return periods (i.e., <10 years and 10-20 years, respectively). In contrast, forests adapt to long drought return periods (>40 years) (Wang-Erlandsson et al., 2016). For this study, we use a uniform 20-year drought return period (following Bouaziz et al., 2020; Nijzink et al., 2016) to avoid any artificially introduced transitions between different ecosystems. Thus, this 20-year drought return period S_r refers to the maximum amount of root zone moisture accessible to vegetation for transpiration during the largest accumulated annual water deficit expected every twenty years under static climate conditions. This we analyse using on the Gumbel extreme value distribution (Gumbel, 1958) and apply it to normalise all $D_{a,y}$. The Gumbel distribution ($F(x)$) is given by:

$$F(x) = \exp\left[-\exp\left[-\frac{(x-\mu)}{\alpha}\right]\right] \tag{A4}$$

Where μ and α are the location and scale parameters, respectively. We calculate this using the python package 'skextremes'(skextremes Documentation):

$$S_r = \overline{D_{a,y}} + K \times \sigma_{n-1} \tag{A5}$$

Where K is the frequency factor given by:

$$K = \frac{y_t - y_n}{S_n} \tag{A6}$$

And y_t is the reduced variate given by:

$$y_t = -\left[\ln\left[\ln\left(\frac{T}{T-1}\right)\right]\right] \tag{A7}$$

Where T is the drought return period (i.e., 20 years used in this study), $\overline{D_{a,y}}$ is the mean annual accumulated deficit for the years 2001-2012, σ_{n-1} is the standard deviation of the sample. Also, y_n is the reduced mean and S_n is the reduced standard deviation, which for n = 11 years (since we are calculating S_r in a hydrological year – simulation starts mid-year – we therefore lose one year) is equal to 0.4996 and 0.9676, respectively (Gumbel, 1958).

Since the CMIP6 (-historical and -SSP estimates, the timeframe considered are 2000-2014 and 2086-2100, respectively) doesn't have daily estimates of evaporation and precipitation for all Earth System Models (ESMs), we directly use the monthly estimates of precipitation and evaporation to modify Eq. (A1) as:

$$D_{t} = E_{t(monthly)} - P_{t(monthly)} \qquad (A8)$$

Here, $t(monthly)$ denotes the month count since the start of the simulation. The rest of the steps (Eq. A2-A7) remain the same for CMIP6 datasets. For CMIP6 runs, y_n and S_n in Eq. (6) are calculated for $n = 14$ years (Eq. A7) equal to 0.5100 and 1.0095, respectively. The S_r estimates derived from daily and monthly empirical estimates (from Eq. A1 and A8) are compared in Fig. S8 to evaluate uncertainty.
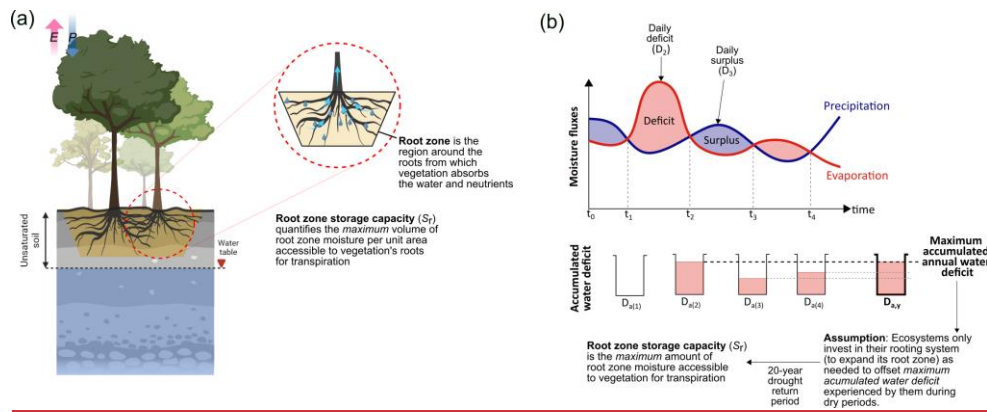
Figure A1: The figure illustrates the root zone storage capacity (S_r) of the ecosystem. (a) We show the difference between the ecosystem's root zone and how that constitutes its S_r. (b) Conceptual illustration of how the ecosystem's precipitation and evaporation fluxes constitute the maximum accumulated annual water deficit ($D_{a,y}$) and S_r. The figure is adopted from Singh (2023) and Wang-Erlandsson et al. (2016).

A2. Abiotic and biotic factors influence soil moisture availability

In this study, S_r quantifies the hydrological buffer necessary for an ecosystem to maintain its structure and functions, reflecting the amount of root zone soil moisture available to vegetation for transpiration. Our mass-balance-based S_r methodology, while not directly distinguishing between the biotic and abiotic influences on soil moisture and root characteristics, does incorporate their critical role in shaping the ecohydrology of the ecosystem under climate change. By utilising empirical precipitation and evaporation data, our approach

theoretically captures the combined impact of these biotic and abiotic factors on the actual hydrological regime (including soil moisture) of the ecosystem (Sect. 2.3.2).

We acknowledge that abiotic factors such as soil texture, structure, and depth profoundly affect soil water-holding capacity (Fayos, 1997). For instance, field studies suggest that clay and organic-rich soils exhibit superior water retention capabilities due to their fine textures and high surface areas, which is crucial to vegetation for moisture uptake during extended dry periods (Bronick and Lal, 2005; Fayos, 1997). Additionally, the depth and porosity of soil also dictate its ability to absorb and store water in the soil, with deeper, less compacted soils providing a higher buffer against drought by allowing greater water infiltration (Indoria et al., 2020; Smith et al., 2001). Climate change, by altering temperature and precipitation patterns, can modify these abiotic soil properties, potentially leading to loss in soil water retention capacity through erosion and compaction (Dexter, 2004)(Dexter, 2004).

Moreover, biotic factors, including plant-root dynamics and microbial activity, also play essential roles in shaping the ecosystem (Brunner et al., 2015; Sveen et al., 2024). Deep and extensive root systems not only directly improve access to deeper soil moisture, but also physically modify the soil to enhance its permeability and storage (Canadell et al., 1996; Jackson et al., 1996). Additionally, microbial processes contribute by breaking down organic matter, thereby improving the soil's structural integrity and ability to retain water (Dittert et al., 2006). These biotic interactions, coupled with changing abiotic factors under climate change, underscore the complex dynamics that govern soil moisture availability and ecosystem resilience. However, this study does not consider the direct impact of future climate change on biotic and abiotic factors, nor their influence on ecosystems, beyond changes to S_{fc}.

905

Figure A2: (a) The figure compares the root zone storage capacity (S_r) with the ecosystem state (i.e., tree cover). This figure expands on the conceptual illustration from Fig. A1, showing how the ecosystem's precipitation and evaporation fluxes contribute to S_r under different forest transition scenarios: (b) forest-savanna transition, (c) transition to a more water-limited state, and (d) reversion to a less water-limited state.

A3. Using precipitation to discern savanna from forests under future climate change

Under future climate change, some ecosystems will remain forest, while others may transition to savanna. In our S_t-based framework, without information about above-ground forest structure, it is difficult to discern whether an ecosystem is a forest or savanna just with S_r (for instance, an ecosystem with S_t of 200 mm can either be a moderately water-limited forest or savanna; Sect. 2.3.2). Differentiating these ecosystems is easier under the current climate, where we have several remote sensing products capturing vegetation structure (e.g., tree cover density, tree height, floristic patterns) (Aleman et al., 2020; Hirota et al., 2011; Xu et al., 2016). However, under future climate, we must find a proxy, since land-use information in ESMs are prescribed (i.e., not biophysically simulated) (Ma et al., 2020).

To address this, previous studies have either relied on vegetation structure proxies provided by ESMs (e.g., net primary productivity) (Boulton et al., 2013; Jones et al., 2009), or assumed that terrestrial ecosystems are in equilibrium with their climate (Staal et al., 2020) (see Supplementary Information). In this study, we adopted the latter approach and utilised climate variables, specifically (bias-corrected) mean annual precipitation and the precipitation seasonality index, as proxies to make this distinction (Fig. S4). The climate conditions (or range) necessary for forest ecosystems to sustain themselves are determined by comparing empirical estimates of mean annual precipitation and precipitation seasonality index with S_t. These estimates are then bias-corrected (following the same methods described in Sect. 2.3.3) before applying them to future climate scenarios. This (revised) classification of terrestrial ecosystems is then used to assess forest transitions under future climate change scenarios.

Appendix B: Results

B1. Sensitivity analysis reveals robust performance of the framework

Sensitivity analysis reveals that ~~Moreover, since the projected transitions are sensitive to ecosystems' hydroclimatic changes and adaptive strategies, we perform sensitivity analyses on S_t (representing S_t-based adaptation) and forest-savanna transition thresholds to check the robustness of the projected transitions (Figs. 1-2 and Supplementary Figs. 18-22). F~~by setting~~ixing~~ an extreme S_t threshold – signifying a forest-savanna transition for ecosystems that cannot maintain their above-ground structure at high S_t – we observe some shifts near the already projected risk regions and coastal areas~~close to the already projected risk regions and coastal regions~~ (Fig. 3 and ~~Supplementary~~ Fig. S18). However, thi~~s~~e transition risk identified in the coastal regions ~~could~~may be an artefact of interpolating hydroclimate estimates to higher resolution~~.~~ Additionally, since evaporation is more prevalent over oceans than land, this could result in high S_t values, thereby projecting an elevated tipping risk in these coastal areas. ~~and since oceans have more prevalent evaporation than land – it could lead to high S_t and, therefore, projection of tipping risk in coastal regions.~~

We also discover that variations in the evaporation datasets and return periods used for calculating S_r have minimal effect on forest transitions (Figs. S19 and S20). Although the forest classification thresholds may shift with different evaporation products under current climate conditions (Singh et al., 2020), our histogram equivalence method ensures that forest classifications under future climates adjust accordingly, resulting in minor alterations to the final outcome (Fig. 1b and Figs. S19-20). Furthermore, while S_r values tend to increase with shorter return periods, the impact of these changes becomes less significant with longer return periods (Wang-Erlandsson et al., 2016); leading to minor variations in the end results (Fig. S20).

Moreover, lowering the forest-savanna transition thresholds can reduce the risk of forest-savanna transition since it expands the associated range of climate conditions (i.e., mean annual precipitation and seasonality) necessary for forests to sustain their structure and functions (Figs. S21-22). Conversely, increasing the forest-savanna transition threshold leads to an opposite trend, where the risk of transition increases (Fig. S22). Despite these sensitivity analyses, the variation in transition magnitudes is minor, and the trends across different SSP scenarios for both continents remain consistent (Fig. 2 and Figs. S18-S22). Therefore, the conclusions drawn from this study remain robust, even with variations in factors that could potentially affect forest transitions.

Data availability

All the data generated during this study is made publicly available at Zenodo: https://zenodo.org/record/7706640. Other datasets that support the findings of this study are publicly available at: (CMIP6; citations referred to in ~~Supplementary~~ Table S2) https://aims2.llnl.gov/, (Root zone storage capacity; empirical) https://github.com/chandrakant6492/Drought-coping-strategy, (P-CHIRPS) https://data.chc.ucsb.edu/products/CHIRPS-2.0/, (E-BESS) ftp://147.46.64.183/, (E-FLUXCOM) ftp.bgc-jena.mpg.de, (E-PML) https://data.csiro.au/collections/#collection/CIcsiro:17375v2, (E-ERA5) https://cds.climate.copernicus.eu/cdsapp#!/dataset/reanalysis-era5-single-levels, (Globcover) http://due.esrin.esa.int/page_globcover.php~~http://due.esrin.esa.int.ezp.sub.su.se/page_globcover.php~~.
Potential transitions for each ESM based on the comparison between empirical (2001-2012) and SSP (2086-2100) scenarios are presented in Supplementary ~~Data~~Information.

Code availability

The python-language scripts used for the analyses presented in this study are available from GitHub: https://github.com/chandrakant6492/Future-forest-transitions-CMIP6. The python-language code for calculating (empirical) root zone storage capacity is available from GitHub: https://github.com/chandrakant6492/Drought-coping-strategy.

Author contributions

All authors contributed to the conceptualisation of this research. CS performed the analyses and wrote the initial draft. All authors contributed to the discussion and revisions, leading to the final version of the manuscript.

Competing interests

The authors declare no competing interests.

References

Ahlström, A., Canadell, J. G., Schurgers, G., Wu, M., Berry, J. A., Guan, K., and Jackson, R. B.: Hydrologic resilience and Amazon productivity, Nature Communications, 8, 387, https://doi.org/10.1038/s41467-017-00306-z, 2017.

Albasha, R., Mailhol, J.-C., and Cheviron, B.: Compensatory uptake functions in empirical macroscopic root water uptake models – Experimental and numerical analysis, Agricultural Water Management, 155, 22–39, https://doi.org/10.1016/j.agwat.2015.03.010, 2015.

Aleman, J. C., Fayolle, A., Favier, C., Staver, A. C., Dexter, K. G., Ryan, C. M., Azihou, A. F., Bauman, D., Beest, M. te, Chidumayo, E. N., Comiskey, J. A., Cromsigt, J. P. G. M., Dessard, H., Doucet, J.-L., Finckh, M., Gillet, J.-F., Gourlet-Fleury, S., Hempson, G. P., Holdo, R. M., Kirunda, B., Kouame, F. N., Mahy, G., Gonçalves, F. M. P., McNicol, I., Quintano, P. N., Plumptre, A. J., Pritchard, R. C., Revermann, R., Schmitt, C. B., Swemmer, A. M., Talila, H., Woollen, E., and Swaine, M. D.: Floristic evidence for alternative biome states in tropical Africa, PNAS, 117, 28183–28190, https://doi.org/10.1073/pnas.2011515117, 2020.

Armstrong McKay, D. I., Staal, A., Abrams, J. F., Winkelmann, R., Sakschewski, B., Loriani, S., Fetzer, I., Cornell, S. E., Rockström, J., and Lenton, T. M.: Exceeding 1.5°C global warming could trigger multiple climate tipping points, Science, 377, eabn7950, https://doi.org/10.1126/science.abn7950, 2022.

Arora, V. K., Seiler, C., Wang, L., and Kou-Giesbrecht, S.: Towards an ensemble-based evaluation of land surface models in light of uncertain forcings and observations, Biogeosciences, 20, 1313–1355, https://doi.org/10.5194/bg-20-1313-2023, 2023.

Baker, J. C. A., Garcia-Carreras, L., Buermann, W., Souza, D. C. de, Marsham, J. H., Kubota, P. Y., Gloor, M., Coelho, C. A. S., and Spracklen, D. V.: Robust Amazon precipitation projections in climate models that capture realistic land–atmosphere interactions, Environ. Res. Lett., 16, 074002, https://doi.org/10.1088/1748-9326/abfb2e, 2021.

Barros, F. de V., Bittencourt, P. R. L., Brum, M., Restrepo-Coupe, N., Pereira, L., Teodoro, G. S., Saleska, S. R., Borma, L. S., Christoffersen, B. O., Penha, D., Alves, L. F., Lima, A. J. N., Carneiro, V. M. C., Gentine, P., Lee, J.-E., Aragão, L. E. O. C., Ivanov, V., Leal, L. S. M., Araujo, A. C., and Oliveira, R. S.: Hydraulic traits explain differential responses of Amazonian forests to the 2015 El Niño-induced drought, New Phytologist, 223, 1253–1266, https://doi.org/10.1111/nph.15909, 2019.

Bauman, D., Fortunel, C., Delhaye, G., Malhi, Y., Cernusak, L. A., Bentley, L. P., Rifai, S. W., Aguirre-Gutiérrez, J., Menor, I. O., Phillips, O. L., McNellis, B. E., Bradford, M., Laurance, S. G. W., Hutchinson, M. F., Dempsey, R., Santos-Andrade, P. E., Ninantay-Rivera, H. R., Chambi Paucar, J. R., and McMahon, S. M.: Tropical tree mortality has increased with rising atmospheric water stress, Nature, 1–6, https://doi.org/10.1038/s41586-022-04737-7, 2022.

de Boer-Euser, T., McMillan, H. K., Hrachowitz, M., Winsemius, H. C., and Savenije, H. H. G.: Influence of soil and climate on root zone storage capacity, Water Resources Research, 52, 2009–2024, https://doi.org/10.1002/2015WR018115, 2016.

Bouaziz, L. J. E., Steele-Dunne, S. C., Schellekens, J., Weerts, A. H., Stam, J., Sprokkereef, E., Winsemius, H. H. C., Savenije, H. H. G., and Hrachowitz, M.: Improved Understanding of the Link Between Catchment-Scale Vegetation Accessible Storage and Satellite-Derived Soil Water Index, Water Resources Research, 56, e2019WR026365, https://doi.org/10.1029/2019WR026365, 2020.

Boulton, C. A., Good, P., and Lenton, T. M.: Early warning signals of simulated Amazon rainforest dieback, Theor Ecol, 6, 373–384, https://doi.org/10.1007/s12080-013-0191-7, 2013.

37

1038 Boulton, C. A., Booth, B. B. B., and Good, P.: Exploring uncertainty of Amazon dieback in a perturbed
1039 parameter Earth system ensemble, Global Change Biology, 23, 5032–5044,
1040 https://doi.org/10.1111/gcb.13733, 2017.

1041 Boulton, C. A., Lenton, T. M., and Boers, N.: Pronounced loss of Amazon rainforest resilience since the early
1042 2000s, Nat. Clim. Chang., 12, 271–278, https://doi.org/10.1038/s41558-022-01287-8, 2022.

1043 Bovolo, C. I., Wagner, T., Parkin, G., Hein-Griggs, D., Pereira, R., and Jones, R.: The Guiana Shield rainforests—
1044 overlooked guardians of South American climate, Environ. Res. Lett., 13, 074029,
1045 https://doi.org/10.1088/1748-9326/aacf60, 2018.

1046 Brienen, R. J. W., Phillips, O. L., Feldpausch, T. R., Gloor, E., Baker, T. R., Lloyd, J., Lopez-Gonzalez, G.,
1047 Monteagudo-Mendoza, A., Malhi, Y., Lewis, S. L., Vásquez Martinez, R., Alexiades, M., Álvarez Dávila, E.,
1048 Alvarez-Loayza, P., Andrade, A., Aragão, L. E. O. C., Araujo-Murakami, A., Arets, E. J. M. M., Arroyo, L., Aymard
1049 C., G. A., Bánki, O. S., Baraloto, C., Barroso, J., Bonal, D., Boot, R. G. A., Camargo, J. L. C., Castilho, C. V., Chama,
1050 V., Chao, K. J., Chave, J., Comiskey, J. A., Cornejo Valverde, F., da Costa, L., de Oliveira, E. A., Di Fiore, A., Erwin,
1051 T. L., Fauset, S., Forsthofer, M., Galbraith, D. R., Grahame, E. S., Groot, N., Hérault, B., Higuchi, N., Honorio
1052 Coronado, E. N., Keeling, H., Killeen, T. J., Laurance, W. F., Laurance, S., Licona, J., Magnussen, W. E., Marimon,
1053 B. S., Marimon-Junior, B. H., Mendoza, C., Neill, D. A., Nogueira, E. M., Núñez, P., Pallqui Camacho, N. C.,
1054 Parada, A., Pardo-Molina, G., Peacock, J., Peña-Claros, M., Pickavance, G. C., Pitman, N. C. A., Poorter, L.,
1055 Prieto, A., Quesada, C. A., Ramírez, F., Ramírez-Angulo, H., Restrepo, Z., Roopsind, A., Rudas, A., Salomão, R.
1056 P., Schwarz, M., Silva, N., Silva-Espejo, J. E., Silveira, M., Stropp, J., Talbot, J., ter Steege, H., Teran-Aguilar, J.,
1057 Terborgh, J., Thomas-Caesar, R., Toledo, M., Torello-Raventos, M., Umetsu, R. K., van der Heijden, G. M. F.,
1058 van der Hout, P., Guimarães Vieira, I. C., Vieira, S. A., Vilanova, E., Vos, V. A., and Zagt, R. J.: Long-term decline
1059 of the Amazon carbon sink, Nature, 519, 344–348, https://doi.org/10.1038/nature14283, 2015.

1060 Bronick, C. J. and Lal, R.: Soil structure and management: a review, Geoderma, 124, 3–22,
1061 https://doi.org/10.1016/j.geoderma.2004.03.005, 2005.

1062 Brooks, P. D., Chorover, J., Fan, Y., Godsey, S. E., Maxwell, R. M., McNamara, J. P., and Tague, C.: Hydrological
1063 partitioning in the critical zone: Recent advances and opportunities for developing transferable understanding
1064 of water cycle dynamics, Water Resources Research, 51, 6973–6987,
1065 https://doi.org/10.1002/2015WR017039, 2015.

1066 Brum, M., Vadeboncoeur, M. A., Ivanov, V., Asbjornsen, H., Saleska, S., Alves, L. F., Penha, D., Dias, J. D.,
1067 Aragão, L. E. O. C., Barros, F., Bittencourt, P., Pereira, L., and Oliveira, R. S.: Hydrological niche segregation
1068 defines forest structure and drought tolerance strategies in a seasonal Amazon forest, Journal of Ecology, 107,
1069 318–333, https://doi.org/10.1111/1365-2745.13022, 2019.

1070 Brunner, I., Herzog, C., Dawes, M. A., Arend, M., and Sperisen, C.: How tree roots respond to drought,
1071 Frontiers in Plant Science, 6, 2015.

1072 Bruno, R. D., Rocha, H. R. da, Freitas, H. C. de, Goulden, M. L., and Miller, S. D.: Soil moisture dynamics in an
1073 eastern Amazonian tropical forest, Hydrological Processes, 20, 2477–2489, https://doi.org/10.1002/hyp.6211,
1074 2006.

1075 Canadell, J., Jackson, R. B., Ehleringer, J. B., Mooney, H. A., Sala, O. E., and Schulze, E.-D.: Maximum rooting
1076 depth of vegetation types at the global scale, Oecologia, 108, 583–595, https://doi.org/10.1007/BF00329030,
1077 1996.

1078 Canadell, J. G., Monteiro, P. M. S., Costa, M. H., Cunha, L. C. D., Cox, P. M., Eliseev, A. V., Henson, S., Ishii, M.,
1079 Jaccard, S., Koven, C., Lohila, A., Patra, P. K., Piao, S., Syampungani, S., Zaehle, S., Zickfeld, K., Alexandrov, G.
1080 A., Bala, G., Bopp, L., Boysen, L., Cao, L., Chandra, N., Ciais, P., Denisov, S. N., Dentener, F. J., Douville, H., Fay,

38

1081   A., Forster, P., Fox-Kemper, B., Friedlingstein, P., Fu, W., Fuss, S., Garçon, V., Gier, B., Gillett, N. P., Gregor, L.,
1082   Haustein, K., Haverd, V., He, J., Hewitt, H. T., Hoffman, F. M., Ilyina, T., Jackson, R., Jones, C., Keller, D. P.,
1083   Kwiatkowski, L., Lamboll, R. D., Lan, X., Laufkötter, C., Quéré, C. L., Lenton, A., Lewis, J., Liddicoat, S.,
1084   Lorenzoni, L., Lovenduski, N., Macdougall, A. H., Mathesius, S., Matthews, D. H., Meinshausen, M., Mokhov, I.
1085   I., Naik, V., Nicholls, Z. R. J., Nurhati, I. S., O'sullivan, M., Peters, G., Pongratz, J., Poulter, B., Sallée, J.-B.,
1086   Saunois, M., Schuur, E. A. G., I.Seneviratne, S., Stavert, A., Suntharalingam, P., Tachiiri, K., Terhaar, J.,
1087   Thompson, R., Tian, H., Turnbull, J., Vicente-Serrano, S. M., Wang, X., Wanninkhof, R. H., Williamson, P.,
1088   Brovkin, V., Feely, R. A., and Lebehot, A. D.: Global Carbon and other Biogeochemical Cycles and Feedbacks,
1089   in: IPCC AR6 WGI, Final Government Distribution, chapter 5, 2021.

1090   Chai, Y., Martins, G., Nobre, C., von Randow, C., Chen, T., and Dolman, H.: Constraining Amazonian land
1091   surface temperature sensitivity to precipitation and the probability of forest dieback, npj Clim Atmos Sci, 4, 1–
1092   7, https://doi.org/10.1038/s41612-021-00162-1, 2021.

1093   Cheng, S., Huang, J., Ji, F., and Lin, L.: Uncertainties of soil moisture in historical simulations and future
1094   projections, Journal of Geophysical Research: Atmospheres, 122, 2239–2253,
1095   https://doi.org/10.1002/2016JD025871, 2017.

1096   Cole, L. E. S., Bhagwat, S. A., and Willis, K. J.: Recovery and resilience of tropical forests after disturbance,
1097   Nature Communications, 5, 3906, https://doi.org/10.1038/ncomms4906, 2014.

1098   Condit, R., Engelbrecht, B. M. J., Pino, D., Pérez, R., and Turner, B. L.: Species distributions in response to
1099   individual soil nutrients and seasonal drought across a community of tropical trees, PNAS, 110, 5064–5068,
1100   https://doi.org/10.1073/pnas.1218042110, 2013.

1101   Cook, K. H. and Vizy, E. K.: Impact of climate change on mid-twenty-first century growing seasons in Africa,
1102   Clim Dyn, 39, 2937–2955, https://doi.org/10.1007/s00382-012-1324-1, 2012.

1103   Cooper, G. S., Willcock, S., and Dearing, J. A.: Regime shifts occur disproportionately faster in larger
1104   ecosystems, Nature Communications, 11, 1175, https://doi.org/10.1038/s41467-020-15029-x, 2020.

1105   skextremes Documentation: https://github.com/kikocorreoso/scikit-extremes.

1106   Cox, P. M., Betts, R. A., Collins, M., Harris, P. P., Huntingford, C., and Jones, C. D.: Amazonian forest dieback
1107   under climate-carbon cycle projections for the 21st century, Theor Appl Climatol, 78, 137–156,
1108   https://doi.org/10.1007/s00704-004-0049-4, 2004.

1109   Dai, A.: Drought under global warming: a review, WIREs Climate Change, 2, 45–65,
1110   https://doi.org/10.1002/wcc.81, 2011.

1111   Davidson, E. A., de Araújo, A. C., Artaxo, P., Balch, J. K., Brown, I. F., C. Bustamante, M. M., Coe, M. T., DeFries,
1112   R. S., Keller, M., Longo, M., Munger, J. W., Schroeder, W., Soares-Filho, B. S., Souza, C. M., and Wofsy, S. C.:
1113   The Amazon basin in transition, Nature, 481, 321–328, https://doi.org/10.1038/nature10717, 2012.

1114   Dexter, A. R.: Soil physical quality: Part II. Friability, tillage, tilth and hard-setting, Geoderma, 120, 215–225,
1115   https://doi.org/10.1016/j.geoderma.2003.09.005, 2004.

1116   Dittert, K., Wätzel, J., and Sattelmacher, B.: Responses of Alnus glutinosa to Anaerobic Conditions -
1117   Mechanisms and Rate of Oxygen Flux into the Roots, Plant Biology, 8, 212–223, https://doi.org/10.1055/s-
1118   2005-873041, 2006.

1119   Doughty, C. E., Keany, J. M., Wiebe, B. C., Rey-Sanchez, C., Carter, K. R., Middleby, K. B., Cheesman, A. W.,
1120   Goulden, M. L., da Rocha, H. R., Miller, S. D., Malhi, Y., Fauset, S., Gloor, E., Slot, M., Oliveras Menor, I., Crous,

39

1121 K. Y., Goldsmith, G. R., and Fisher, J. B.: Tropical forests are approaching critical temperature thresholds,
1122 Nature, 621, 105–111, https://doi.org/10.1038/s41586-023-06391-z, 2023.

1123 Drijfhout, S., Bathiany, S., Beaulieu, C., Brovkin, V., Claussen, M., Huntingford, C., Scheffer, M., Sgubin, G., and
1124 Swingedouw, D.: Catalogue of abrupt shifts in Intergovernmental Panel on Climate Change climate models,
1125 Proceedings of the National Academy of Sciences, 112, E5777–E5786,
1126 https://doi.org/10.1073/pnas.1511451112, 2015.

1127 Dunning, C. M., Black, E., and Allan, R. P.: Later Wet Seasons with More Intense Rainfall over Africa under
1128 Future Climate Change, Journal of Climate, 31, 9719–9738, 2018.

1129 van der Ent, R. J., Savenije, H. H. G., Schaefli, B., and Steele-Dunne, S. C.: Origin and fate of atmospheric
1130 moisture over continents, Water Resources Research, 46, https://doi.org/10.1029/2010WR009127, 2010.

1131 GlobCover land-use map: http://due.esrin.esa.int/page_globcover.php, last access: 27 February 2022.

1132 Esquivel-Muelbert, A., Baker, T. R., Dexter, K. G., Lewis, S. L., Brienen, R. J. W., Feldpausch, T. R., Lloyd, J.,
1133 Monteagudo-Mendoza, A., Arroyo, L., Álvarez-Dávila, E., Higuchi, N., Marimon, B. S., Marimon-Junior, B. H.,
1134 Silveira, M., Vilanova, E., Gloor, E., Malhi, Y., Chave, J., Barlow, J., Bonal, D., Cardozo, N. D., Erwin, T., Fauset,
1135 S., Hérault, B., Laurance, S., Poorter, L., Qie, L., Stahl, C., Sullivan, M. J. P., Steege, H. ter, Vos, V. A., Zuidema,
1136 P. A., Almeida, E., Oliveira, E. A. de, Andrade, A., Vieira, S. A., Aragão, L., Araujo-Murakami, A., Arets, E., C, G.
1137 A. A., Baraloto, C., Camargo, P. B., Barroso, J. G., Bongers, F., Boot, R., Camargo, J. L., Castro, W., Moscoso, V.
1138 C., Comiskey, J., Valverde, F. C., Costa, A. C. L. da, Pasquel, J. del A., Fiore, A. D., Duque, L. F., Elias, F., Engel, J.,
1139 Llampazo, G. F., Galbraith, D., Fernández, R. H., Coronado, E. H., Hubau, W., Jimenez-Rojas, E., Lima, A. J. N.,
1140 Umetsu, R. K., Laurance, W., Lopez-Gonzalez, G., Lovejoy, T., Cruz, O. A. M., Morandi, P. S., Neill, D., Vargas, P.
1141 N., Camacho, N. C. P., Gutierrez, A. P., Pardo, G., Peacock, J., Peña-Claros, M., Peñuela-Mora, M. C., Petronelli,
1142 P., Pickavance, G. C., Pitman, N., Prieto, A., Quesada, C., Ramírez-Angulo, H., Réjou-Méchain, M., Correa, Z. R.,
1143 Roopsind, A., Rudas, A., Salomão, R., Silva, N., Espejo, J. S., Singh, J., Stropp, J., Terborgh, J., Thomas, R.,
1144 Toledo, M., Torres-Lezama, A., Gamarra, L. V., Meer, P. J. van de, Heijden, G. van der, et al.: Compositional
1145 response of Amazon forests to climate change, Global Change Biology, 25, 39–56,
1146 https://doi.org/10.1111/gcb.14413, 2019.

1147 Fan, Y., Miguez-Macho, G., Jobbágy, E. G., Jackson, R. B., and Otero-Casal, C.: Hydrologic regulation of plant
1148 rooting depth, Proceedings of the National Academy of Sciences, 114, 10572–10577,
1149 https://doi.org/10.1073/pnas.1712381114, 2017.

1150 Fayos, C. B.: The roles of texture and structure in the water retention capacity of burnt Mediterranean soils
1151 with varying rainfall, CATENA, 31, 219–236, https://doi.org/10.1016/S0341-8162(97)00041-6, 1997.

1152 Ferreira, D., Marshall, J., and Rose, B.: Climate Determinism Revisited: Multiple Equilibria in a Complex
1153 Climate Model, Journal of Climate, 24, 992–1012, https://doi.org/10.1175/2010JCLI3580.1, 2011.

1154 Fleischer, K., Rammig, A., De Kauwe, M. G., Walker, A. P., Domingues, T. F., Fuchslueger, L., Garcia, S., Goll, D.
1155 S., Grandis, A., Jiang, M., Haverd, V., Hofhansl, F., Holm, J. A., Kruijt, B., Leung, F., Medlyn, B. E., Mercado, L.
1156 M., Norby, R. J., Pak, B., von Randow, C., Quesada, C. A., Schaap, K. J., Valverde-Barrantes, O. J., Wang, Y.-P.,
1157 Yang, X., Zaehle, S., Zhu, Q., and Lapola, D. M.: Amazon forest response to CO2 fertilization dependent on
1158 plant phosphorus acquisition, Nat. Geosci., 12, 736–741, https://doi.org/10.1038/s41561-019-0404-9, 2019.

1159 Flores, B. M., Montoya, E., Sakschewski, B., Nascimento, N., Staal, A., Betts, R. A., Levis, C., Lapola, D. M.,
1160 Esquível-Muelbert, A., Jakovac, C., Nobre, C. A., Oliveira, R. S., Borma, L. S., Nian, D., Boers, N., Hecht, S. B., ter
1161 Steege, H., Arieira, J., Lucas, I. L., Berenguer, E., Marengo, J. A., Gatti, L. V., Mattos, C. R. C., and Hirota, M.:
1162 Critical transitions in the Amazon forest system, Nature, 626, 555–564, https://doi.org/10.1038/s41586-023-
1163 06970-0, 2024.

1164 Funk, C., Peterson, P., Landsfeld, M., Pedreros, D., Verdin, J., Shukla, S., Husak, G., Rowland, J., Harrison, L.,
1165 Hoell, A., and Michaelsen, J.: The climate hazards infrared precipitation with stations—a new environmental
1166 record for monitoring extremes, Scientific Data, 2, 150066, https://doi.org/10.1038/sdata.2015.66, 2015.

1167 Gao, H., Hrachowitz, M., Schymanski, S. J., Fenicia, F., Sriwongsitanon, N., and Savenije, H. H. G.: Climate
1168 controls how ecosystems size the root zone storage capacity at catchment scale: Root zone storage capacity in
1169 catchments, Geophysical Research Letters, 41, 7916–7923, https://doi.org/10.1002/2014GL061668, 2014.

1170 Grimm, N. B., Chapin III, F. S., Bierwagen, B., Gonzalez, P., Groffman, P. M., Luo, Y., Melton, F., Nadelhoffer, K.,
1171 Pairis, A., Raymond, P. A., Schimel, J., and Williamson, C. E.: The impacts of climate change on ecosystem
1172 structure and function, Frontiers in Ecology and the Environment, 11, 474–482,
1173 https://doi.org/10.1890/120282, 2013.

1174 Gumbel, E. J.: Statistics of extremes., Columbia University Press, New York, 1958.

1175 Guswa, A. J.: The influence of climate on root depth: A carbon cost-benefit analysis, Water Resources
1176 Research, 44, W02427, https://doi.org/10.1029/2007WR006384, 2008.

1177 Hahm, W. J., Rempe, D. M., Dralle, D. N., Dawson, T. E., Lovill, S. M., Bryk, A. B., Bish, D. L., Schieber, J., and
1178 Dietrich, W. E.: Lithologically Controlled Subsurface Critical Zone Thickness and Water Storage Capacity
1179 Determine Regional Plant Community Composition, Water Resources Research, 55, 3028–3055,
1180 https://doi.org/10.1029/2018WR023760, 2019.

1181 Hall, A., Cox, P., Huntingford, C., and Klein, S.: Progressing emergent constraints on future climate change,
1182 Nat. Clim. Chang., 9, 269–278, https://doi.org/10.1038/s41558-019-0436-6, 2019.

1183 Hersbach, H., Bell, B., Berrisford, P., Hirahara, S., Horányi, A., Muñoz-Sabater, J., Nicolas, J., Peubey, C., Radu,
1184 R., Schepers, D., Simmons, A., Soci, C., Abdalla, S., Abellan, X., Balsamo, G., Bechtold, P., Biavati, G., Bidlot, J.,
1185 Bonavita, M., Chiara, G. D., Dahlgren, P., Dee, D., Diamantakis, M., Dragani, R., Flemming, J., Forbes, R.,
1186 Fuentes, M., Geer, A., Haimberger, L., Healy, S., Hogan, R. J., Hólm, E., Janisková, M., Keeley, S., Laloyaux, P.,
1187 Lopez, P., Lupu, C., Radnoti, G., Rosnay, P. de, Rozum, I., Vamborg, F., Villaume, S., and Thépaut, J.-N.: The
1188 ERA5 Global Reanalysis, Quarterly Journal of the Royal Meteorological Society, 245, 111840,
1189 https://doi.org/10.1002/qj.3803, 2020.

1190 Higgins, S. I. and Scheiter, S.: Atmospheric CO_2 forces abrupt vegetation shifts locally, but not globally, Nature,
1191 488, 209–212, https://doi.org/10.1038/nature11238, 2012.

1192 Hildebrandt, A., Kleidon, A., and Bechmann, M.: A thermodynamic formulation of root water uptake,
1193 Hydrology and Earth System Sciences, 20, 3441–3454, https://doi.org/10.5194/hess-20-3441-2016, 2016.

1194 Hirota, M., Holmgren, M., Van Nes, E. H., and Scheffer, M.: Global Resilience of Tropical Forest and Savanna to
1195 Critical Transitions, Science, 334, 232–235, https://doi.org/10.1126/science.1210657, 2011.

1196 Hirota, M., Flores, B. M., Betts, R., Borma, L. S., Esquivel-Muelbert, A., Jakovac, C., Lapola, D. M., Montoya, E.,
1197 Oliveira, R. S., and Sakschewski, B.: Chapter 24: Resilience of the Amazon forest to global changes: Assessing
1198 the risk of tipping points, in: Amazon Assessment Report 2021, edited by: Nobre, C., Encalada, A., Anderson,
1199 E., Roca Alcazar, F. H., Bustamante, M., Mena, C., Peña-Claros, M., Poveda, G., Rodriguez, J. P., Saleska, S.,
1200 Trumbore, S. E., Val, A., Villa Nova, L., Abramovay, R., Alencar, A., Rodriguez Alzza, A. C., Armenteras, D.,
1201 Artaxo, P., Athayde, S., Barretto Filho, H. T., Barlow, J., Berenguer, E., Bortolotto, F., Costa, F. de A., Costa, M.
1202 H., Cuvi, N., Fearnside, P., Ferreira, J., Flores, B. M., Frieri, S., Gatti, L. V., Guayasamin, J. M., Hecht, S., Hirota,
1203 M., Hoorn, C., Josse, C., Lapola, D. M., Larrea, C., Larrea-Alcazar, D. M., Lehm Ardaya, Z., Malhi, Y., Marengo, J.
1204 A., Melack, J., Moraes R., M., Moutinho, P., Murmis, M. R., Neves, E. G., Paez, B., Painter, L., Ramos, A.,

Rosero-Peña, M. C., Schmink, M., Sist, P., ter Steege, H., Val, P., van der Voort, H., Varese, M., and Zapata-Ríos, G., UN Sustainable Development Solutions Network (SDSN), https://doi.org/10.55161/QPYS9758, 2021.

Hofhansl, F., Andersen, K. M., Fleischer, K., Fuchslueger, L., Rammig, A., Schaap, K. J., Valverde-Barrantes, O. J., and Lapola, D. M.: Amazon Forest Ecosystem Responses to Elevated Atmospheric CO2 and Alterations in Nutrient Availability: Filling the Gaps with Model-Experiment Integration, Frontiers in Earth Science, 4, 2016.

Hubau, W., Lewis, S. L., Phillips, O. L., Affum-Baffoe, K., Beeckman, H., Cuní-Sanchez, A., Daniels, A. K., Ewango, C. E. N., Fauset, S., Mukinzi, J. M., Sheil, D., Sonké, B., Sullivan, M. J. P., Sunderland, T. C. H., Taedoumg, H., Thomas, S. C., White, L. J. T., Abernethy, K. A., Adu-Bredu, S., Amani, C. A., Baker, T. R., Banin, L. F., Baya, F., Begne, S. K., Bennett, A. C., Benedet, F., Bitariho, R., Bocko, Y. E., Boeckx, P., Boundja, P., Brienen, R. J. W., Brncic, T., Chezeaux, E., Chuyong, G. B., Clark, C. J., Collins, M., Comiskey, J. A., Coomes, D. A., Dargie, G. C., de Haulleville, T., Kamdem, M. N. D., Doucet, J.-L., Esquivel-Muelbert, A., Feldpausch, T. R., Fofanah, A., Foli, E. G., Gilpin, M., Gloor, E., Gonmadje, C., Gourlet-Fleury, S., Hall, J. S., Hamilton, A. C., Harris, D. J., Hart, T. B., Hockemba, M. B. N., Hladik, A., Ifo, S. A., Jeffery, K. J., Jucker, T., Yakusu, E. K., Kearsley, E., Kenfack, D., Koch, A., Leal, M. E., Levesley, A., Lindsell, J. A., Lisingo, J., Lopez-Gonzalez, G., Lovett, J. C., Makana, J.-R., Malhi, Y., Marshall, A. R., Martin, J., Martin, E. H., Mbayu, F. M., Medjibe, V. P., Mihindou, V., Mitchard, E. T. A., Moore, S., Munishi, P. K. T., Bengone, N. N., Ojo, L., Ondo, F. E., Peh, K. S.-H., Pickavance, G. C., Poulsen, A. D., Poulsen, J. R., Qie, L., Reitsma, J., Rovero, F., Swaine, M. D., Talbot, J., Taplin, J., Taylor, D. M., Thomas, D. W., Toirambe, B., Mukendi, J. T., Tuagben, D., Umunay, P. M., et al.: Asynchronous carbon sink saturation in African and Amazonian tropical forests, Nature, 579, 80–87, https://doi.org/10.1038/s41586-020-2035-0, 2020.

Huntingford, C., Zelazowski, P., Galbraith, D., Mercado, L. M., Sitch, S., Fisher, R., Lomas, M., Walker, A. P., Jones, C. D., Booth, B. B. B., Malhi, Y., Hemming, D., Kay, G., Good, P., Lewis, S. L., Phillips, O. L., Atkin, O. K., Lloyd, J., Gloor, E., Zaragoza-Castells, J., Meir, P., Betts, R., Harris, P. P., Nobre, C., Marengo, J., and Cox, P. M.: Simulated resilience of tropical rainforests to CO2-induced climate change, Nature Geosci, 6, 268–273, https://doi.org/10.1038/ngeo1741, 2013.

Hurtt, G. C., Chini, L., Sahajpal, R., Frolking, S., Bodirsky, B. L., Calvin, K., Doelman, J. C., Fisk, J., Fujimori, S., Klein Goldewijk, K., Hasegawa, T., Havlik, P., Heinimann, A., Humpenöder, F., Jungclaus, J., Kaplan, J. O., Kennedy, J., Krisztin, T., Lawrence, D., Lawrence, P., Ma, L., Mertz, O., Pongratz, J., Popp, A., Poulter, B., Riahi, K., Shevliakova, E., Stehfest, E., Thornton, P., Tubiello, F. N., van Vuuren, D. P., and Zhang, X.: Harmonization of global land use change and management for the period 850–2100 (LUH2) for CMIP6, Geoscientific Model Development, 13, 5425–5464, https://doi.org/10.5194/gmd-13-5425-2020, 2020.

Indoria, A. K., Sharma, K. L., and Reddy, K. S.: Chapter 18 - Hydraulic properties of soil under warming climate, in: Climate Change and Soil Interactions, edited by: Prasad, M. N. V. and Pietrzykowski, M., Elsevier, 473–508, https://doi.org/10.1016/B978-0-12-818032-7.00018-7, 2020.

Jach, L., Warrach-Sagi, K., Ingwersen, J., Kaas, E., and Wulfmeyer, V.: Land Cover Impacts on Land-Atmosphere Coupling Strength in Climate Simulations With WRF Over Europe, Journal of Geophysical Research: Atmospheres, 125, e2019JD031989, https://doi.org/10.1029/2019JD031989, 2020.

Jackson, R. B., Canadell, J., Ehleringer, J. R., Mooney, H. A., Sala, O. E., and Schulze, E. D.: A global analysis of root distributions for terrestrial biomes, Oecologia, 108, 389–411, https://doi.org/10.1007/BF00333714, 1996.

Jehn, F. U., Kemp, L., Ilin, E., Funk, C., Wang, J. R., and Breuer, L.: Focus of the IPCC Assessment Reports Has Shifted to Lower Temperatures, Earth's Future, 10, e2022EF002876, https://doi.org/10.1029/2022EF002876, 2022.

1248 Jiang, C. and Ryu, Y.: Multi-scale evaluation of global gross primary productivity and evapotranspiration
1249 products derived from Breathing Earth System Simulator (BESS), Remote Sensing of Environment, 186, 528–
1250 547, https://doi.org/10.1016/j.rse.2016.08.030, 2016.

1251 Jones, C., Lowe, J., Liddicoat, S., and Betts, R.: Committed terrestrial ecosystem changes due to climate
1252 change, Nature Geosci, 2, 484–487, https://doi.org/10.1038/ngeo555, 2009.

1253 Jung, M., Koirala, S., Weber, U., Ichii, K., Gans, F., Camps-Valls, G., Papale, D., Schwalm, C., Tramontana, G.,
1254 and Reichstein, M.: The FLUXCOM ensemble of global land-atmosphere energy fluxes, Sci Data, 6, 74,
1255 https://doi.org/10.1038/s41597-019-0076-8, 2019.

1256 Koch, A., Hubau, W., and Lewis, S. L.: Earth System Models Are Not Capturing Present-Day Tropical Forest
1257 Carbon Dynamics, Earth's Future, 9, e2020EF001874, https://doi.org/10.1029/2020EF001874, 2021.

1258 Kooperman, G. J., Chen, Y., Hoffman, F. M., Koven, C. D., Lindsay, K., Pritchard, M. S., Swann, A. L. S., and
1259 Randerson, J. T.: Forest response to rising CO2 drives zonally asymmetric rainfall change over tropical land,
1260 Nature Clim Change, 8, 434–440, https://doi.org/10.1038/s41558-018-0144-7, 2018.

1261 Körner, C.: A matter of tree longevity, Science, 355, 130–131, https://doi.org/10.1126/science.aal2449, 2017.

1262 Küçük, Ç., Koirala, S., Carvalhais, N., Miralles, D. G., Reichstein, M., and Jung, M.: Characterizing the Response
1263 of Vegetation Cover to Water Limitation in Africa Using Geostationary Satellites, Journal of Advances in
1264 Modeling Earth Systems, 14, e2021MS002730, https://doi.org/10.1029/2021MS002730, 2022.

1265 Kukal, M. S. and Irmak, S.: Can limits of plant available water be inferred from soil moisture distributions?,
1266 Agricultural & Environmental Letters, 8, e20113, https://doi.org/10.1002/ael2.20113, 2023.

1267 Lammertsma, E. I., Boer, H. J. de, Dekker, S. C., Dilcher, D. L., Lotter, A. F., and Wagner-Cremer, F.: Global CO2
1268 rise leads to reduced maximum stomatal conductance in Florida vegetation, PNAS, 108, 4035–4040,
1269 https://doi.org/10.1073/pnas.1100371108, 2011.

1270 Lawrence, D., Coe, M., Walker, W., Verchot, L., and Vandecar, K.: The Unseen Effects of Deforestation:
1271 Biophysical Effects on Climate, Frontiers in Forests and Global Change, 5, 2022.

1272 Leite-Filho, A. T., Soares-Filho, B. S., Davis, J. L., Abrahão, G. M., and Börner, J.: Deforestation reduces rainfall
1273 and agricultural revenues in the Brazilian Amazon, Nat Commun, 12, 2591, https://doi.org/10.1038/s41467-
1274 021-22840-7, 2021.

1275 Lenton, T. M.: Early warning of climate tipping points, Nature Clim Change, 1, 201–209,
1276 https://doi.org/10.1038/nclimate1143, 2011.

1277 Lewis, S. L., Edwards, D. P., and Galbraith, D.: Increasing human dominance of tropical forests, Science, 349,
1278 827–832, https://doi.org/10.1126/science.aaa9932, 2015.

1279 Li, Y., Brando, P. M., Morton, D. C., Lawrence, D. M., Yang, H., and Randerson, J. T.: Deforestation-induced
1280 climate change reduces carbon storage in remaining tropical forests, Nat Commun, 13, 1964,
1281 https://doi.org/10.1038/s41467-022-29601-0, 2022.

1282 Liu, W., Sun, F., Lim, W. H., Zhang, J., Wang, H., Shiogama, H., and Zhang, Y.: Global drought and severe
1283 drought-affected populations in 1.5 and 2 °C warmer worlds, Earth System Dynamics, 9, 267–283,
1284 https://doi.org/10.5194/esd-9-267-2018, 2018.

1285 Liu, Y., Kumar, M., Katul, G. G., Feng, X., and Konings, A. G.: Plant hydraulics accentuates the effect of
1286 atmospheric moisture stress on transpiration, Nat. Clim. Chang., 10, 691–695,
1287 https://doi.org/10.1038/s41558-020-0781-5, 2020.

1288 Ma, L., Hurtt, G. C., Chini, L. P., Sahajpal, R., Pongratz, J., Frolking, S., Stehfest, E., Klein Goldewijk, K., O'Leary,
1289 D., and Doelman, J. C.: Global rules for translating land-use change (LUH2) to land-cover change for CMIP6
1290 using GLM2, Geoscientific Model Development, 13, 3203–3220, https://doi.org/10.5194/gmd-13-3203-2020,
1291 2020.

1292 Malhi, Y., Roberts, J. T., Betts, R. A., Killeen, T. J., Li, W., and Nobre, C. A.: Climate Change, Deforestation, and
1293 the Fate of the Amazon, Science, 319, 169–172, https://doi.org/10.1126/science.1146961, 2008.

1294 Malhi, Y., Gardner, T. A., Goldsmith, G. R., Silman, M. R., and Zelazowski, P.: Tropical Forests in the
1295 Anthropocene, Annu. Rev. Environ. Resour., 39, 125–159, https://doi.org/10.1146/annurev-environ-030713-
1296 155141, 2014.

1297 Mamalakis, A., Randerson, J. T., Yu, J.-Y., Pritchard, M. S., Magnusdottir, G., Smyth, P., Levine, P. A., Yu, S., and
1298 Foufoula-Georgiou, E.: Zonally contrasting shifts of the tropical rain belt in response to climate change, Nature
1299 Climate Change, 11, 143–151, https://doi.org/10.1038/s41558-020-00963-x, 2021.

1300 Maslin, M. and Austin, P.: Climate models at their limit?, Nature, 486, 183–184,
1301 https://doi.org/10.1038/486183a, 2012.

1302 McCormick, E. L., Dralle, D. N., Hahm, W. J., Tune, A. K., Schmidt, L. M., Chadwick, K. D., and Rempe, D. M.:
1303 Widespread woody plant use of water stored in bedrock, Nature, 597, 225–229,
1304 https://doi.org/10.1038/s41586-021-03761-3, 2021.

1305 McFarlane, N.: Parameterizations: representing key processes in climate models without resolving them,
1306 WIREs Climate Change, 2, 482–497, https://doi.org/10.1002/wcc.122, 2011.

1307 Nepstad, D. C., Verssimo, A., Alencar, A., Nobre, C., Lima, E., Lefebvre, P., Schlesinger, P., Potter, C., Moutinho,
1308 P., Mendoza, E., Cochrane, M., and Brooks, V.: Large-scale impoverishment of Amazonian forests by logging
1309 and fire, Nature, 398, 505–508, https://doi.org/10.1038/19066, 1999.

1310 van Nes, E. H., Arani, B. M. S., Staal, A., van der Bolt, B., Flores, B. M., Bathiany, S., and Scheffer, M.: What Do
1311 You Mean, 'Tipping Point'?, Trends in Ecology & Evolution, 31, 902–904,
1312 https://doi.org/10.1016/j.tree.2016.09.011, 2016.

1313 Nijzink, R., Hutton, C., Pechlivanidis, I., Capell, R., Arheimer, B., Freer, J., Han, D., Wagener, T., McGuire, K.,
1314 Savenije, H., and Hrachowitz, M.: The evolution of root-zone moisture capacities after deforestation: a step
1315 towards hydrological predictions under change?, Hydrology and Earth System Sciences, 20, 4775–4799,
1316 https://doi.org/10.5194/hess-20-4775-2016, 2016.

1317 Nippert, J. B. and Holdo, R. M.: Challenging the maximum rooting depth paradigm in grasslands and savannas,
1318 Functional Ecology, 29, 739–745, https://doi.org/10.1111/1365-2435.12390, 2015.

1319 Nof, D.: Simple Versus Complex Climate Modeling, Eos, Transactions American Geophysical Union, 89, 544–
1320 545, https://doi.org/10.1029/2008EO520006, 2008.

1321 Oliveira, R. S., Dawson, T. E., Burgess, S. S. O., and Nepstad, D. C.: Hydraulic redistribution in three Amazonian
1322 trees, Oecologia, 145, 354–363, https://doi.org/10.1007/s00442-005-0108-2, 2005.

Parry, I. M., Ritchie, P. D. L., and Cox, P. M.: Evidence of localised Amazon rainforest dieback in CMIP6 models, Earth System Dynamics, 13, 1667–1675, https://doi.org/10.5194/esd-13-1667-2022, 2022.

Pascale, S., Carvalho, L. M. V., Adams, D. K., Castro, C. L., and Cavalcanti, I. F. A.: Current and Future Variations of the Monsoons of the Americas in a Warming Climate, Curr Clim Change Rep, 5, 125–144, https://doi.org/10.1007/s40641-019-00135-w, 2019.

Piani, C., Weedon, G. P., Best, M., Gomes, S. M., Viterbo, P., Hagemann, S., and Haerter, J. O.: Statistical bias correction of global simulated daily precipitation and temperature for the application of hydrological models, Journal of Hydrology, 395, 199–215, https://doi.org/10.1016/j.jhydrol.2010.10.024, 2010.

Poorter, L., Bongers, F., Aide, T. M., Almeyda Zambrano, A. M., Balvanera, P., Becknell, J. M., Boukili, V., Brancalion, P. H. S., Broadbent, E. N., Chazdon, R. L., Craven, D., de Almeida-Cortez, J. S., Cabral, G. A. L., de Jong, B. H. J., Denslow, J. S., Dent, D. H., DeWalt, S. J., Dupuy, J. M., Durán, S. M., Espírito-Santo, M. M., Fandino, M. C., César, R. G., Hall, J. S., Hernandez-Stefanoni, J. L., Jakovac, C. C., Junqueira, A. B., Kennard, D., Letcher, S. G., Licona, J.-C., Lohbeck, M., Marín-Spiotta, E., Martínez-Ramos, M., Massoca, P., Meave, J. A., Mesquita, R., Mora, F., Muñoz, R., Muscarella, R., Nunes, Y. R. F., Ochoa-Gaona, S., de Oliveira, A. A., Orihuela-Belmonte, E., Peña-Claros, M., Pérez-García, E. A., Piotto, D., Powers, J. S., Rodríguez-Velázquez, J., Romero-Pérez, I. E., Ruíz, J., Saldarriaga, J. G., Sanchez-Azofeifa, A., Schwartz, N. B., Steininger, M. K., Swenson, N. G., Toledo, M., Uriarte, M., van Breugel, M., van der Wal, H., Veloso, M. D. M., Vester, H. F. M., Vicentini, A., Vieira, I. C. G., Bentos, T. V., Williamson, G. B., and Rozendaal, D. M. A.: Biomass resilience of Neotropical secondary forests, Nature, 530, 211–214, https://doi.org/10.1038/nature16512, 2016.

Rammig, A.: Tropical carbon sinks are saturating at different times on different continents, Nature, 579, 38–39, https://doi.org/10.1038/d41586-020-00423-8, 2020.

Reyer, C. P. O., Brouwers, N., Rammig, A., Brook, B. W., Epila, J., Grant, R. F., Holmgren, M., Langerwisch, F., Leuzinger, S., Lucht, W., Medlyn, B., Pfeifer, M., Steinkamp, J., Vanderwel, M. C., Verbeeck, H., and Villela, D. M.: Forest resilience and tipping points at different spatio-temporal scales: approaches and challenges, Journal of Ecology, 103, 5–15, https://doi.org/10.1111/1365-2745.12337, 2015.

Rosas, T., Mencuccini, M., Barba, J., Cochard, H., Saura-Mas, S., and Martínez-Vilalta, J.: Adjustments and coordination of hydraulic, leaf and stem traits along a water availability gradient, New Phytologist, 223, 632–646, https://doi.org/10.1111/nph.15684, 2019.

Schenk, H. J.: Soil depth, plant rooting strategies and species' niches, New Phytologist, 178, 223–225, https://doi.org/10.1111/j.1469-8137.2008.02427.x, 2008.

Schenk, H. J. and Jackson, R. B.: The Global Biogeography of Roots, Ecological Monographs, 72, 311–328, https://doi.org/10.1890/0012-9615(2002)072[0311:TGBOR]2.0.CO;2, 2002.

Schumacher, D. L., Keune, J., Dirmeyer, P., and Miralles, D. G.: Drought self-propagation in drylands due to land–atmosphere feedbacks, Nat. Geosci., 15, 262–268, https://doi.org/10.1038/s41561-022-00912-7, 2022.

Singh, C.: Rooting for forest resilience : Implications of climate and land-use change on the tropical rainforests, 2023.

Singh, C., Wang-Erlandsson, L., Fetzer, I., Rockström, J., and van der Ent, R.: Rootzone storage capacity reveals drought coping strategies along rainforest-savanna transitions, Environ. Res. Lett., 15, 124021, https://doi.org/10.1088/1748-9326/abc377, 2020.

Singh, C., van der Ent, R., Wang-Erlandsson, L., and Fetzer, I.: Hydroclimatic adaptation critical to the resilience of tropical forests, Global Change Biology, 28, 2930–2939, https://doi.org/10.1111/gcb.16115, 2022.

1364 Slik, J. W. F., Franklin, J., Arroyo-Rodríguez, V., Field, R., Aguilar, S., Aguirre, N., Ahumada, J., Aiba, S.-I., Alves,
1365 L. F., K, A., Avella, A., Mora, F., Aymard C., G. A., Báez, S., Balvanera, P., Bastian, M. L., Bastin, J.-F., Bellingham,
1366 P. J., van den Berg, E., da Conceição Bispo, P., Boeckx, P., Boehning-Gaese, K., Bongers, F., Boyle, B.,
1367 Brambach, F., Brearley, F. Q., Brown, S., Chai, S.-L., Chazdon, R. L., Chen, S., Chhang, P., Chuyong, G., Ewango,
1368 C., Coronado, I. M., Cristóbal-Azkarate, J., Culmsee, H., Damas, K., Dattaraja, H. S., Davidar, P., DeWalt, S. J.,
1369 Din, H., Drake, D. R., Duque, A., Durigan, G., Eichhorn, K., Eler, E. S., Enoki, T., Ensslin, A., Fandohan, A. B.,
1370 Farwig, N., Feeley, K. J., Fischer, M., Forshed, O., Garcia, Q. S., Garkoti, S. C., Gillespie, T. W., Gillet, J.-F.,
1371 Gonmadje, C., Granzow-de la Cerda, I., Griffith, D. M., Grogan, J., Hakeem, K. R., Harris, D. J., Harrison, R. D.,
1372 Hector, A., Hemp, A., Homeier, J., Hussain, M. S., Ibarra-Manríquez, G., Hanum, I. F., Imai, N., Jansen, P. A.,
1373 Joly, C. A., Joseph, S., Kartawinata, K., Kearsley, E., Kelly, D. L., Kessler, M., Killeen, T. J., Kooyman, R. M.,
1374 Laumonier, Y., Laurance, S. G., Laurance, W. F., Lawes, M. J., Letcher, S. G., Lindsell, J., Lovett, J., Lozada, J., Lu,
1375 X., Lykke, A. M., Mahmud, K. B., Mahayani, N. P. D., Mansor, A., Marshall, A. R., Martin, E. H., Calderado Leal
1376 Matos, D., Meave, J. A., Melo, F. P. L., Mendoza, Z. H. A., et al.: Phylogenetic classification of the world's
1377 tropical forests, Proceedings of the National Academy of Sciences, 115, 1837–1842,
1378 https://doi.org/10.1073/pnas.1714977115, 2018.

1379 Smith, C. W., Johnston, M. A., and Lorentz, S. A.: The effect of soil compaction on the water retention
1380 characteristics of soils in forest plantations, South African Journal of Plant and Soil, 18, 87–97,
1381 https://doi.org/10.1080/02571862.2001.10634410, 2001.

1382 Staal, A., Tuinenburg, O. A., Bosmans, J. H. C., Holmgren, M., van Nes, E. H., Scheffer, M., Zemp, D. C., and
1383 Dekker, S. C.: Forest-rainfall cascades buffer against drought across the Amazon, Nature Climate Change, 8,
1384 539–543, https://doi.org/10.1038/s41558-018-0177-y, 2018.

1385 Staal, A., Fetzer, I., Wang-Erlandsson, L., Bosmans, J. H. C., Dekker, S. C., van Nes, E. H., Rockström, J., and
1386 Tuinenburg, O. A.: Hysteresis of tropical forests in the 21st century, Nat Commun, 11, 4978,
1387 https://doi.org/10.1038/s41467-020-18728-7, 2020.

1388 Still, C. J., Berry, J. A., Collatz, G. J., and DeFries, R. S.: Global distribution of C3 and C4 vegetation: Carbon
1389 cycle implications, Global Biogeochemical Cycles, 17, 6-1-6–14, https://doi.org/10.1029/2001GB001807,
1390 2003.

1391 Stocker, B. D., Tumber-Dávila, S. J., Konings, A. G., Anderson, M. C., Hain, C., and Jackson, R. B.: Global
1392 patterns of water storage in the rooting zones of vegetation, Nat. Geosci., 1–7,
1393 https://doi.org/10.1038/s41561-023-01125-2, 2023.

1394 Sveen, T. R., Hannula, S. E., and Bahram, M.: Microbial regulation of feedbacks to ecosystem change, Trends in
1395 Microbiology, 32, 68–78, https://doi.org/10.1016/j.tim.2023.06.006, 2024.

1396 Trumbore, S., Brando, P., and Hartmann, H.: Forest health and global change, Science, 349, 814–818,
1397 https://doi.org/10.1126/science.aac6759, 2015.

1398 Valdes, P.: Built for stability, Nature Geosci, 4, 414–416, https://doi.org/10.1038/ngeo1200, 2011.

1399 Wang, E., Smith, C. J., Wang, E., and Smith, C. J.: Modelling the growth and water uptake function of plant
1400 root systems: a review, Aust. J. Agric. Res., 55, 501–523, https://doi.org/10.1071/AR03201, 2004.

1401 Wang-Erlandsson, L., Bastiaanssen, W. G. M., Gao, H., Jägermeyr, J., Senay, G. B., van Dijk, A. I. J. M.,
1402 Guerschman, J. P., Keys, P. W., Gordon, L. J., and Savenije, H. H. G.: Global root zone storage capacity from
1403 satellite-based evaporation, Hydrology and Earth System Sciences, 20, 1459–1481,
1404 https://doi.org/10.5194/hess-20-1459-2016, 2016.

1405 Wang-Erlandsson, L., Tobian, A., van der Ent, R. J., Fetzer, I., te Wierik, S., Porkka, M., Staal, A., Jaramillo, F.,
1406 Dahlmann, H., Singh, C., Greve, P., Gerten, D., Keys, P. W., Gleeson, T., Cornell, S. E., Steffen, W., Bai, X., and
1407 Rockström, J.: A planetary boundary for green water, Nat Rev Earth Environ, 3, 380–392,
1408 https://doi.org/10.1038/s43017-022-00287-8, 2022.

1409 Wolfe, B. T., Sperry, J. S., and Kursar, T. A.: Does leaf shedding protect stems from cavitation during seasonal
1410 droughts? A test of the hydraulic fuse hypothesis, New Phytologist, 212, 1007–1018,
1411 https://doi.org/10.1111/nph.14087, 2016.

1412 Wunderling, N., Staal, A., Sakschewski, B., Hirota, M., Tuinenburg, O. A., Donges, J. F., Barbosa, H. M. J., and
1413 Winkelmann, R.: Recurrent droughts increase risk of cascading tipping events by outpacing adaptive capacities
1414 in the Amazon rainforest, Proceedings of the National Academy of Sciences, 119, e2120777119,
1415 https://doi.org/10.1073/pnas.2120777119, 2022.

1416 Xie, S.-P., Deser, C., Vecchi, G. A., Ma, J., Teng, H., and Wittenberg, A. T.: Global Warming Pattern Formation:
1417 Sea Surface Temperature and Rainfall, Journal of Climate, 23, 966–986,
1418 https://doi.org/10.1175/2009JCLI3329.1, 2010.

1419 Xu, C., Hantson, S., Holmgren, M., van Nes, E. H., Staal, A., and Scheffer, M.: Remotely sensed canopy height
1420 reveals three pantropical ecosystem states, Ecology, 97, 2518–2521, https://doi.org/10.1002/ecy.1470, 2016.

1421 Xue, B.-L., Guo, Q., Otto, A., Xiao, J., Tao, S., and Li, L.: Global patterns, trends, and drivers of water use
1422 efficiency from 2000 to 2013, Ecosphere, 6, art174, https://doi.org/10.1890/ES14-00416.1, 2015.

1423 Yang, Y., Saatchi, S. S., Xu, L., Yu, Y., Choi, S., Phillips, N., Kennedy, R., Keller, M., Knyazikhin, Y., and Myneni, R.
1424 B.: Post-drought decline of the Amazon carbon sink, Nat Commun, 9, 3172, https://doi.org/10.1038/s41467-
1425 018-05668-6, 2018.

1426 Yu, Z., Chen, X., Zhou, G., Agathokleous, E., Li, L., Liu, Z., Wu, J., Zhou, P., Xue, M., Chen, Y., Yan, W., Liu, L., Shi,
1427 T., and Zhao, X.: Natural forest growth and human induced ecosystem disturbance influence water yield in
1428 forests, Commun Earth Environ, 3, 148, https://doi.org/10.1038/s43247-022-00483-w, 2022.

1429 Yuan, K., Zhu, Q., Riley, W. J., Li, F., and Wu, H.: Understanding and reducing the uncertainties of land surface
1430 energy flux partitioning within CMIP6 land models, Agricultural and Forest Meteorology, 319, 108920,
1431 https://doi.org/10.1016/j.agrformet.2022.108920, 2022.

1432 Zemp, D. C., Schleussner, C.-F., Barbosa, H. M. J., van der Ent, R. J., Donges, J. F., Heinke, J., Sampaio, G., and
1433 Rammig, A.: On the importance of cascading moisture recycling in South America, Atmospheric Chemistry and
1434 Physics, 14, 13337–13359, https://doi.org/10.5194/acp-14-13337-2014, 2014.

1435 Zemp, D. C., Schleussner, C.-F., Barbosa, H. M. J., Hirota, M., Montade, V., Sampaio, G., Staal, A., Wang-
1436 Erlandsson, L., and Rammig, A.: Self-amplified Amazon forest loss due to vegetation-atmosphere feedbacks,
1437 Nature Communications, 8, 14681, https://doi.org/10.1038/ncomms14681, 2017.

1438 Zhang, Y., Peña-Arancibia, J. L., McVicar, T. R., Chiew, F. H. S., Vaze, J., Liu, C., Lu, X., Zheng, H., Wang, Y., Liu, Y.
1439 Y., Miralles, D. G., and Pan, M.: Multi-decadal trends in global terrestrial evapotranspiration and its
1440 components, Scientific Reports, 6, 19124, https://doi.org/10.1038/srep19124, 2016.

1441 Zilli, M. T., Carvalho, L. M. V., and Lintner, B. R.: The poleward shift of South Atlantic Convergence Zone in
1442 recent decades, Clim Dyn, 52, 2545–2563, https://doi.org/10.1007/s00382-018-4277-1, 2019.

1443